REFERENCES

Attanasi, O.A., D'Auria, M., Emanuele, L., Favi, G., Filippone, P., Mantellini, F., Pucciariello, R., Racioppi, R., (2008) Synthesis of new polyazine by 1,4 photochemical or anionic polymerization of 1.2-diaza-1.3-butadiene. European Polymer Journal, 44, 2545-3550.

Barra, G.M.O., Matins, R.R., Kafer, K.A., Paniago, R., Vasques, C.T., Pires, A.T.N., (2008) Thermoplastic elastomer/polyaniline blends: Evaluation of mechanical and electromechanical properties. Polymer Testing 27, 886–892.

Bassil, M., Davenas, J., Tahchi, M.EL, (2008) Electrochemical properties and actuationmechanisms of polyacrylamide hydrogel for artificial muscle application. Sensors and Actuators B, 134, 496-501.

Behl, M., Lendlein, A., (2007) Shape-memory polymers. Materailstoday, 10 (4), 20-48.

Boden, N., Bissell, R., Clements, J., and Movaghar, B. (1996) Discotic liquid crystals – Self-organizing molecule wires. Current Sciences, 71, 599

C. Gerbo, Future Materials "Technology for Competitive Advantage". TechTarget, Australian National University, March 2004.

Chaloner-Gill, B., Cheer, C. J., Roberts, J. E., Euler, W. B., (1990) Structure of Glyoxal Dihydrazone and Synthesis, Characterization, and Iodine Doping of Unsubstituted Polyazine. Macromolecules, 23, 4597-4603.

Cladis, P.E. (2001) Phase Transition in Liquid Crystalline Elastomers: A fundamental Aspect of LCEs as artificial Muscle. Advanced Liquid Crystal Technologies. POB 1314, 1-8.

C.R. Nave, Department of Physics and Astronomy, Georgia State University, 2005.

Davydov, B.Ĕ., Drabkin, I.A., Korshak, Yu.v. and Rozenshtein, L.D. (1963) Electrophysical properties of polyazines. Izvestiya Akademii Nauk SSSR, Seriya Khimicheskaya, 1521-1523

Dudis, D.S., Yeates, A.T., Kost, D., Smith, D.A., Medrano, J., (1993) Iodine-doped polyazine: evidence against bipolarons and nitrenium ions. J. Am. Chem. Soc., 115, 8770-8774.

"Electroactive Polymers-EAPs." 16-19 Apr. 2001. The A to Z materials. < http://www.azom.com/details.asp/ArticleID=885 >

Euler, W.B. (1990) Synthesis, characterization, and iodine doping of a soluble polyazine: the propyl-methyl substituted derivative. Chem. Mater., 2. 209-213

Euler, W.B. (1996) IR spectroscopy of Pristine and Iodine-Doped Permethylpolyazine. Chem. Mater., 8(2), 554-557.

Gazotti, Jr W.A., Faez, R., Paoli, M.D., (1999) Thermal and mechanical behavior of a conductive elastomeric blend based on a soluble polyaniline derivative. European Polymer Journal, 35, 35-40.

Geerts, Y.H. "Discotics liquid crystals as electron carrier materials." ULB. 5 July 2002. < http://www.imec.be/tcmwebapp/internet/course.tcm >

Gill, B.C., Cheer, C.J., Roberts, J.E., and Euler, W.B. (1990) Structure of Glyoxal Dihydrazone and Synthesis, Characterization, and Iodine Doping of Unsubstituted Polyazine. Macromolecules, 23, 4597-4603.

Ginic-Markovic., Dutta N.K., Dimopoulus M., Roy Choudhury N., Matisons J.G. (2000) Viscoelastic behavior of filled, and unfilled, EPDM elastomer. Thermochimica Acta, 211-216.

Hanato, M., Kambara, S., and Okamoto, S., (1961) Jornal of Polymer Science, 51, S26.

Hauer, C.R., King, G.S., McCool, E.L., Euler, W.B., Ferrara, J.D., and Youngs, W.J. (1987) Structure 0f 2,3-butanedione dihydrazone and IR study of higher polyazine: a new class of polymeric conductors. J. Am. Chem. Soc., 109, 5760-5765.

J.D. Nam, H.R. Choi, J.C. Koo, Y.K. Lee, K.J. Kim, Dielectric Elastomers for Artificial Muscles, Engineering, 2007, pp. 37-48.

J. Feher, G. Filipcsei, J. Szalma, and M. Zrinyi (2001) Bending deformation of neutral polymer gels induced by electric fields, Colloids and Surfaces A: Physicochemical and Engineering Aspects, 183–185, 505–515.

J. Kyokane, H. Ishimoto, H. Yugen, T. Hirai, T.Ueda and K.Yoshino (1999) Electro-striction effect of polyurethane elastomer (PUE) and its application to actuators, Synthetic Metals, 103, 2366-2367.

J. Sebastein Plante, S. Dubowsky (2007) On the performance mechanism of Dielectric Elastomer Actuators, Sensor and Actuator, 137, 96-109.

Ladegaard, A., Larsen, P.S. (2008) Physical and chemical properties of dielectric elastomers, 25-32.

L. Hao, Z. Shi, X.zhao (2009) Mechanical behavior of starch/silicone oil/silicone rubber hybrid electric elastomer, Reactive&Function Polymers 69, 165-169.

K. Urayama, K. Kondo, Y.O. Arai, T. Takigawa (2005) Electrically driven deformations of nematic gels, Journal Article, 71.

Li, M.H., and Keller, P. (2006) Artificia muscles based on liquid crystal elastomers. Phil. Trans. R. Soc. A, 364, 3763-2777.

Li, Z., Zhang J., Chen S. (2009) Effect of carbon blacks with various structure on electrical properties of filled ethylene-propylene-diene rubber. Journal of Electrostatics, 67, 73-75

L.W. Liu, J.M. Fan, Z. Zhang, L. Shi, Y. J. Lin, J. S. Leng (2008) Analysis of the Novel Strain Responsive Actuators of Silicone Dielectric Elastomer, Advanced Materials Research, 47-50, 298-301.

Madden, J., (2005) Artificial Muscle Technology. IEEE Journal of Oceanic Engineering, 29(3), 706.

M. Rubinstein, R.H. Colby, Polymer Physics, Oxford University Press, New York, 2003.

Nero, J.D., Laks B., (1997) A comparative study of ordered and disordered distribution of defects in polyazine derivatives. Synthetic Metals, 84, 423-424.

Pratt, C. "Conducting Polymer." 22 Feb. 1996.
< http://homepage.ntlworld.com/colin.pratt/cpoly.pdf>

R. Kunanuruksapong, A. Sirivat (2008) Electrical properties and electromechanical responses of acrylic elastomers and styrene copolymers: effect of temperature, Applied Physics A 92, 313-320.

R. Pelrine, R. Kornbluh, J. Joseph, R. Heydt, Q. Pei, S. Chiba (2000) Compressive Stress Accumulation in Composite Nanoporous Gold and Silicone Bilayer Membranes: Underlying Mechanisms and Remedies, Mater. Sci. Eng. C 11 395, 89–100. 396.

See, H., Sakurai, R., Saito, T., Asai, S., Sumita, M., (2001) Relationship between electric current and matrix modulus in electrorheological elastomers. Journal of Electrostatics 50, 303-312.

Shankar, R., Ghosh, T.K., Spontak, R.J., (2009) Mechanical and actuation behavior of electroactive nanostructured polymers. Sensors and Actuators A, 151, 46-52

Sidorov, T.A., Komarova, L.I., Korshak, Yu.V., and Davydov, B.Ĕ. (1967) Infrared spectra and structure of polyazine. Izvestiya Akademii Nauk SSSR, Seriya Khimicheskaya, 531-534.

Shirakawa, H., Louis, E.J., MacDiarmid, A.G., Chiang, C.K., and Heegee, A.J., (1977) Journal of Chem. Soc. Chem Commun, 578

Spillmann, C.M., Naciri, J.,Martin, B.D., Farahat, W., Herr, H., Ratna, B.R. (2007) Stacking nematic elastomers for artificial muscle application. Sensors amd Actuators A, 133, 500-505.

Tarachiwin, L., Kiattibutr, P., Ruangchuay, L., Sirivat, A., Schwank, J., (2002) Electrical conductivity response of polyaniline films to ethanol-water mixtures. Synthetic Metals, 129, 303-308.

T. Puvanatvattana, D. Chotpattananont, P. Hiamtup, S. Niamlang, A. Sirivat, A.M. Jamieson (2006) Electric field induced stress moduli in polythiophene/polyisoprene elastomer blends. Reactive & Functional Polymers, 66, 1575–1588.

Thomsen, D.L., Keller, P., Naciri, J., Pink, R., Joen, H., Shenoy, D., amd Ratna, B.R. (2001) Liquid Crystal Elastomers with Mechanical Properties of a Muscle. Macromolecules, 34 (17), 5868-5875.

Urayama, K. (2007) Selected Issues in Liquid Crystal Elastomers and Gel. Macromolecules, 40(7), 2277-2278.

Wichiansee, W., Sirivat, A., (2009) Electrorheological properties of poly(dimethylsiloxane) and poly(3,4-ethylenedioxythiophene)/poly(stylene sulfonic acid)/ethylene glycol blends. Materials Science and Engineering C 29, 78–84.

Wissler, M., Mazza, E., (2007) Electromechanical coupling in dielectric elastomer actuators. Sensors and Actuators A 138, 384–393.

APPENDICES

Appendix A Correction Factor (K) Measurement

A two point probe meter connected with a source power supplier (Keithley/ Model 6517A) was employed to determine the electrical conductivity of materials. A constant voltage was applied and the current was simultaneously measured. According to the geometric effects of the probe, the geometrical correction factor depends on the configuration and probe tip spacing:

$$K = w/l \tag{A.1}$$

where K is the geometric correction factor, w is the probe width or the tip spacing (cm), and l is the probe length (cm).

The geometric correction factor can be determined by using standard materials whose specific resistivity values are known. In our case, silicon wafer chips were used as the standard materials. The resistance was measured by using our custom-made two-point probe, obtained by applying various voltages and simultaneously measuring currents. The geometric correction factor was calculated via the equation:

$$K = \rho/R \times t = I \times \rho/V \times t \tag{A.2}$$

where ρ is the resistivity of a standard silicon wafer (Ω.cm), R is the resistance of film (Ω), t is the film thickness (cm), I is the measured current (A) ,and V is the applied voltage (V).

Table A1 Voltage-current data of the probe number 1 calibration with Si-wafer whose sheet resistivity of 107.373 Ω/sq, 25°C, 60-65 %RH

V			Current (A)			K=I/V*ρ/t		
100	100	100	0.01068	0.010963	0.011083	0.011467	0.011772	0.0119
90	90	90	0.011224	0.011251	0.011222	0.01339	0.013423	0.013388
80	80	80	0.011265	0.011356	0.011296	0.015119	0.015242	0.015161
70	70	70	0.011377	0.011472	0.011492	0.017451	0.017597	0.017627
60	60	60	0.011465	0.011495	0.011541	0.020517	0.020571	0.020654
50	50	50	0.011504	0.011532	0.011549	0.024704	0.024764	0.0248
40	40	40	0.007358	0.006376	0.005797	0.019752	0.017114	0.015562
30	30	30	0.002436	0.002194	0.00201	0.00872	0.007852	0.007196
20	20	20	0.000493	0.000461	0.000446	0.002647	0.002474	0.002395
10	10	10	4.7E-05	4.59E-05	4.24E-05	0.000505	0.000493	0.000455
9	9	9	3.18E-05	2.99E-05	2.93E-05	0.000379	0.000357	0.00035
8	8	8	2.31E-05	2.2E-05	2.11E-05	0.00031	0.000295	0.000283
7	7	7	1.5E-05	6.43E-06	4.68E-06	0.000229	9.86E-05	7.18E-05
6	6	6	3.42E-06	3.4E-06	3.44E-06	6.12E-05	6.08E-05	6.15E-05
5	5	5	2.76E-06	2.84E-06	2.82E-06	5.92E-05	6.1E-05	6.05E-05
4	4	4	2.22E-06	2.04E-06	1.81E-06	5.97E-05	5.47E-05	4.86E-05
3	3	3	1.45E-06	1.42E-06	1.42E-06	5.19E-05	5.09E-05	5.09E-05
2	2	2	1.07E-06	1.02E-06	1.05E-06	5.75E-05	5.49E-05	5.61E-05
1	1	1	5.89E-07	5.67E-07	5.71E-07	6.32E-05	6.09E-05	6.13E-05
0.9	0.9	0.9	4.63E-07	4.66E-07	4.72E-07	5.52E-05	5.56E-05	5.63E-05
0.8	0.8	0.8	3.93E-07	3.96E-07	3.85E-07	5.28E-05	5.32E-05	5.17E-05

V			Current (A)			K=I/V*ρ/t		
0.7	0.7	0.7	3.17E-07	3.07E-07	3.03E-07	4.87E-05	4.71E-05	4.64E-05
0.6	0.6	0.6	2.27E-07	2.2E-07	2.23E-07	4.07E-05	3.93E-05	3.98E-05
0.5	0.5	0.5	1.59E-07	1.62E-07	1.63E-07	3.42E-05	3.47E-05	3.5E-05
0.4	0.4	0.4	1.07E-07	1.06E-07	1.04E-07	2.88E-05	2.84E-05	2.8E-05
0.3	0.3	0.3	6.82E-08	6.74E-08	6.66E-08	2.44E-05	2.41E-05	2.38E-05
0.2	0.2	0.2	3.7E-08	3.66E-08	3.72E-08	1.99E-05	1.96E-05	2E-05
0.1	0.1	0.1	1.62E-08	1.61E-08	1.6E-08	1.74E-05	1.73E-05	1.71E-05
0.05	0.05	0.05	7.63E-09	7.66E-09	7.63E-09	1.64E-05	1.65E-05	1.64E-05
0.01	0.01	0.01	1.47E-09	2.07E-09	8.98E-10	1.57E-05	2.22E-05	9.64E-06

Correction factor (K)				
1	**2**	**3**	**Avg.**	**SD**
0.0026	0.00257	0.00255	0.00257	2.31023E-05

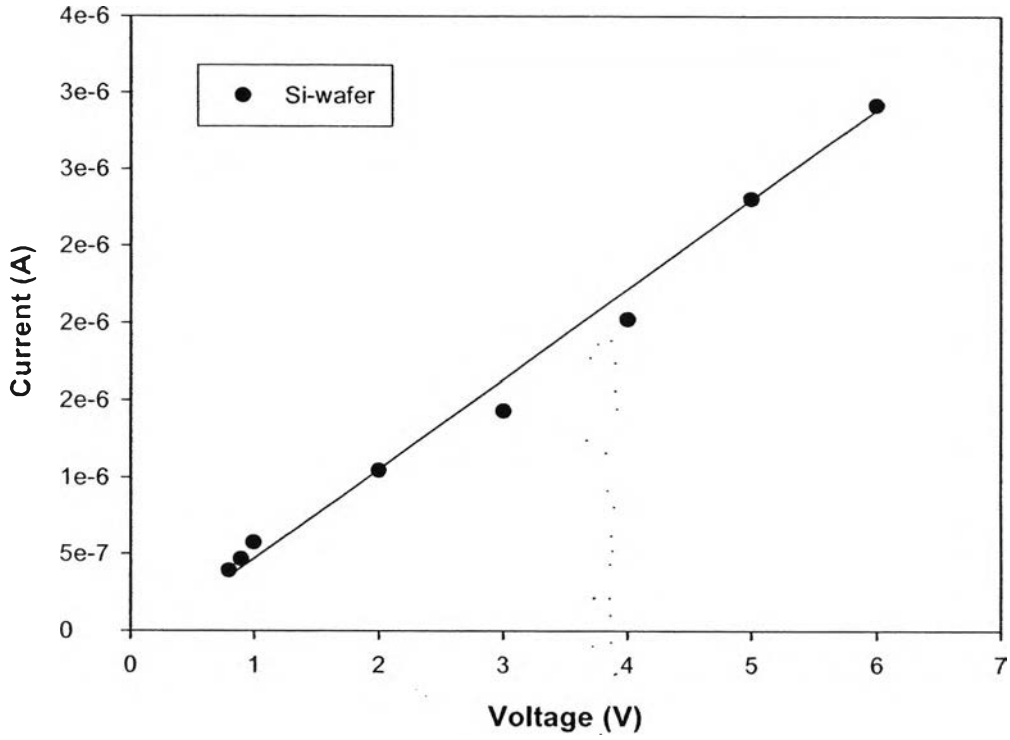

Figure A1 Voltage vs. current data of the probe number 1 calibration with Si-wafer whose sheet resistivity of 107.373 Ω/sq, 25°C, 60-65 %RH.

Appendix B Conductivity Measurement

The electrical conductivity (σ) can be measured by using the two-point probe mater connected with a voltage supplier (Keithley, 6517A) whose constant voltage can be varied and the current is measured. The conductivity measurement was performed under atmospheric pressure, 40-60 %RH and at 25-27°C. The regime where responsive current is linearly proportional to the applied voltage is called the linear Ohmic regime. The voltage and the current in the regime were converted to the electrical conductivity by the following equation:

$$\sigma = 1/\rho = 1/(R \times t) = I/(R_s \times V \times t) \qquad \text{(B.1)}$$

where σ is the specific conductivity (S/cm), ρ is the specific resistivity (Ω.cm), R_s is the sheet resistance (Ω/sq), t is the thickness of sample pellet (cm), V is the applied voltage (Voltage drop)(V), I is the measured current (A), and K is the geometric correction factor of the two-point probe meter. All sample thicknesses were measured by using a thickness gauge.

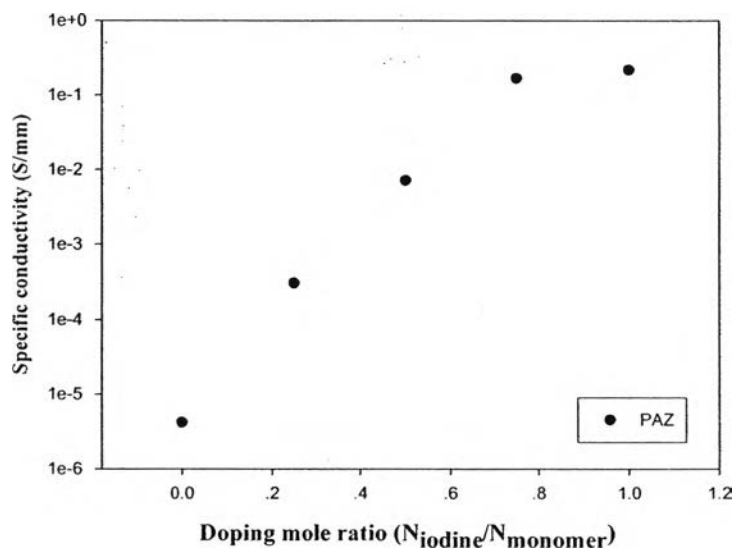

Figure B1 specific conductivity versus doping moles ratio ($N_{iodine}/N_{monomer}$) of PAZ.

Table B1 Voltage-current data in linear regime of De_PAZ at 25°C, 60-65 %RH

Voltage (V)			Current (A)			Specific conductivity (S/cm)		
1	2	3	1	2	3	1	2	3
10	10	10	1E-10	1E-10	1E-10	1E-05	1.1E-05	1.1E-05
9	9	9	9.5E-11	9.2E-11	9.1E-11	1.1E-05	1.1E-05	1E-05
8	8	8	7.9E-11	8E-11	8.1E-11	1E-05	1E-05	1E-05
7	7	7	6.9E-11	7.1E-11	7.2E-11	1E-05	1.1E-05	1.1E-05
6	6	6	6.4E-11	6.4E-11	6.4E-11	1.1E-05	1.1E-05	1.1E-05
5	5	5	5.2E-11	5.2E-11	5.2E-11	1.1E-05	1.1E-05	1.1E-05
4	4	4	1.8E-11	3.1E-11	4.2E-11	4.5E-06	8E-06	1.1E-05
3	3	3	1.3E-11	1.4E-11	1.4E-11	4.5E-06	4.7E-06	4.7E-06
2	2	2	7.8E-12	7.9E-12	7.8E-12	4E-06	4E-06	4E-06
1	1	1	4.1E-12	4E-12	4E-12	4.2E-06	4.1E-06	4.1E-06
0.9	0.9	0.9	3.7E-12	3.7E-12	3.7E-12	4.2E-06	4.2E-06	4.3E-06
0.8	0.8	0.8	3.5E-12	3.4E-12	3.1E-12	4.5E-06	4.4E-06	4E-06
0.7	0.7	0.7	2.8E-12	3.1E-12	3.1E-12	4.1E-06	4.5E-06	4.5E-06
0.6	0.6	0.6	1.5E-12	2.6E-12	2.6E-12	2.6E-06	4.4E-06	4.5E-06
0.5	0.5	0.5	2.1E-12	2.5E-12	2.5E-12	4.3E-06	5.2E-06	5.1E-06
0.4	0.4	0.4	1.6E-12	1.7E-12	1.7E-12	4E-06	4.5E-06	4.3E-06
0.3	0.3	0.3	1.4E-12	1.4E-12	1.4E-12	4.7E-06	4.9E-06	4.9E-06
0.2	0.2	0.2	1.2E-12	1E-12	9.9E-13	6.2E-06	5.2E-06	5.1E-06
0.1	0.1	0.1	-4E-13	-8E-14	-1E-13	-4E-06	-8E-07	-1E-06
0.05	0.05	0.05	-4E-13	-4E-13	-4E-13	-9E-06	-7E-06	-8E-06
0.01	0.01	0.01	1.7E-12	-4E-13	3.3E-13	0.00018	-5E-05	3.4E-05

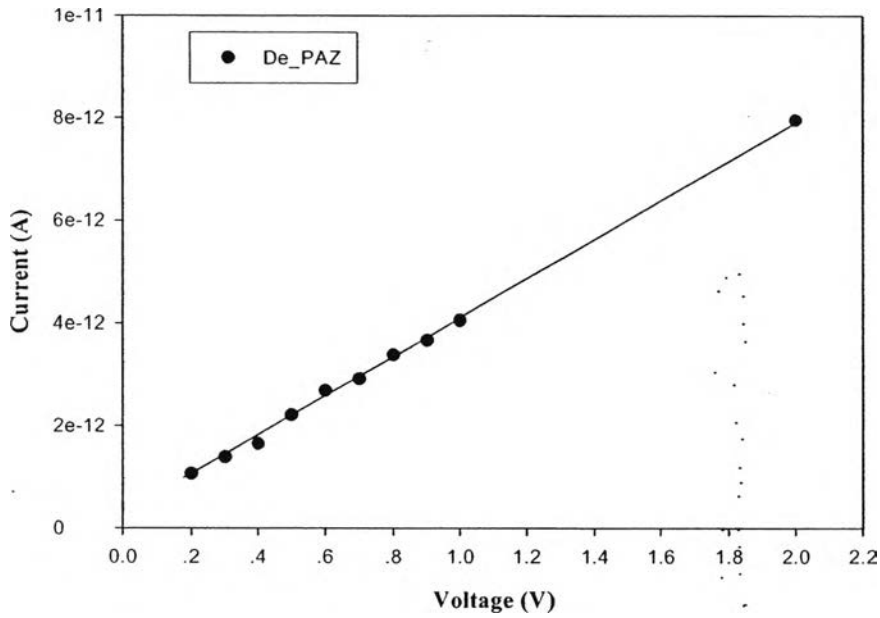

Figure B2 The Ohmic regime of De_PAZ at thickness = 0.01508 cm, 25°C, 60-65 %RH.

Table B2 Voltage-current data in linear regime of D_PAZ 1:1 at 25°C, 60-65 %RH

Voltage (V)			Current (A)			Specific conductivity (S/cm)		
1	2	3	1	2	3	1	2	3
10	10	10	2.55E-06	2.55E-06	2.56E-06	0.071998	0.072115	0.072121
9	9	9	2.29E-06	2.3E-06	2.32E-06	0.071829	0.072154	0.072878
8	8	8	2.05E-06	2.05E-06	2.05E-06	0.072501	0.072235	0.072449
7	7	7	1.79E-06	1.79E-06	1.78E-06	0.072258	0.071999	0.071908
6	6	6	1.55E-06	1.53E-06	1.53E-06	0.072723	0.0722	0.072165
5	5	5	1.28E-06	1.29E-06	1.3E-06	0.072529	0.073065	0.07325
4	4	4	1.04E-06	1.04E-06	1.04E-06	0.073208	0.073193	0.073107
3	3	3	7.76E-07	7.72E-07	7.71E-07	0.073058	0.072672	0.072548
2	2	2	5.22E-07	5.2E-07	5.19E-07	0.073631	0.073386	0.073263
1	1	1	2.6E-07	2.6E-07	2.6E-07	0.073397	0.073528	0.073518
0.9	0.9	0.9	2.35E-07	2.35E-07	2.35E-07	0.073661	0.073705	0.073644
0.8	0.8	0.8	2.08E-07	2.07E-07	2.07E-07	0.073369	0.073112	0.073028
0.7	0.7	0.7	1.81E-07	1.82E-07	1.81E-07	0.07295	0.07325	0.073054
0.6	0.6	0.6	1.55E-07	1.55E-07	1.54E-07	0.07284	0.072725	0.072466
0.5	0.5	0.5	1.28E-07	1.29E-07	1.29E-07	0.072424	0.072568	0.0726
0.4	0.4	0.4	1.03E-07	1.03E-07	1.03E-07	0.072775	0.072682	0.072587
0.3	0.3	0.3	7.71E-08	7.68E-08	7.65E-08	0.072548	0.072254	0.071977
0.2	0.2	0.2	5.11E-08	5.1E-08	5.1E-08	0.072102	0.071972	0.071953
0.1	0.1	0.1	2.61E-08	2.63E-08	2.62E-08	0.073559	0.074225	0.073978
0.05	0.05	0.05	1.35E-08	1.35E-08	1.33E-08	0.076481	0.075934	0.075274
0.01	0.01	0.01	4.7E-09	4.66E-09	4.67E-09	0.132705	0.131403	0.13192

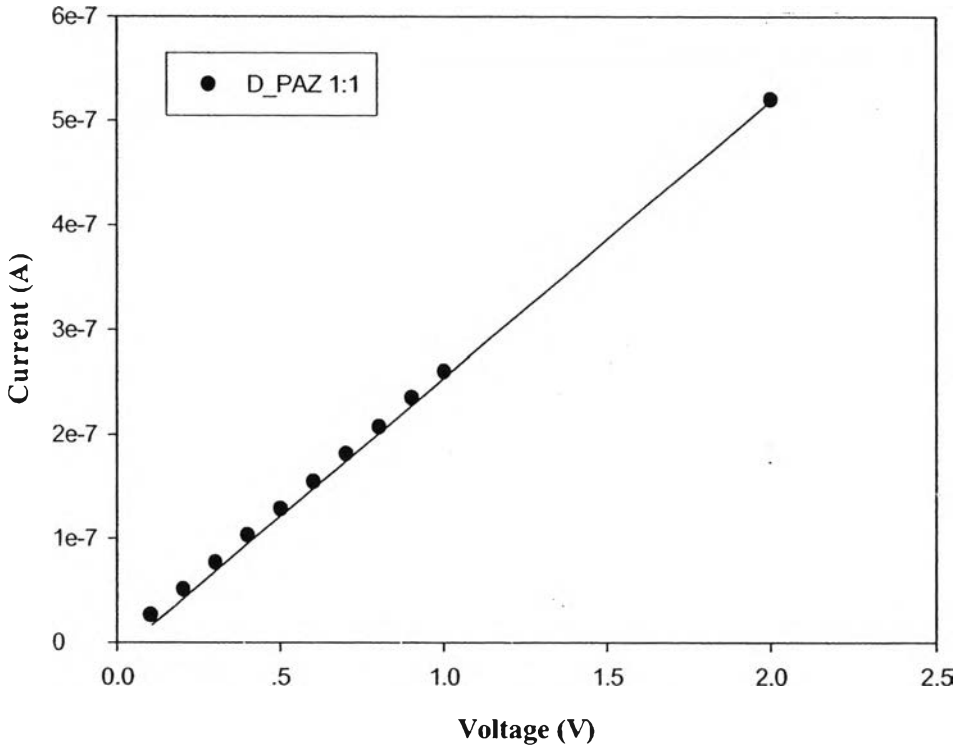

Figure B3 The Ohmic regime of D_PAZ 1:1 at thickness = 0.05501 cm, 25°C, 60-65 %RH.

Table B3 Voltage-current data in linear regime of D_PAZ 0.75:1 at 25°C, 60-65 %RH

Voltage (V)			Current (A)			Specific conductivity (S/cm)		
1	2	3	1	2	3	1	2	3
10	10	10	1.69E-06	1.72E-06	1.74E-06	1.35E-01	1.38E-01	1.39E-01
9	9	9	1.57E-06	1.58E-06	1.59E-06	1.40E-01	1.40E-01	1.41E-01
8	8	8	1.42E-06	1.43E-06	1.43E-06	1.42E-01	1.43E-01	1.43E-01
7	7	7	1.26E-06	1.26E-06	1.27E-06	1.44E-01	1.44E-01	1.45E-01
6	6	6	1.09E-06	1.09E-06	1.10E-06	1.45E-01	1.46E-01	1.46E-01
5	5	5	9.14E-07	9.17E-07	9.20E-07	1.46E-01	1.47E-01	1.47E-01
4	4	4	7.41E-07	7.44E-07	7.46E-07	1.48E-01	1.49E-01	1.49E-01
3	3	3	5.62E-07	5.63E-07	5.66E-07	1.50E-01	1.50E-01	1.51E-01
2	2	2	3.78E-07	3.80E-07	3.81E-07	1.51E-01	1.52E-01	1.52E-01
1	1	1	1.90E-07	1.91E-07	1.91E-07	1.52E-01	1.53E-01	1.53E-01
0.9	0.9	0.9	1.72E-07	1.73E-07	1.73E-07	1.53E-01	1.53E-01	1.54E-01
0.8	0.8	0.8	1.54E-07	1.55E-07	1.55E-07	1.54E-01	1.55E-01	1.55E-01
0.7	0.7	0.7	1.36E-07	1.36E-07	1.37E-07	1.55E-01	1.56E-01	1.56E-01
0.6	0.6	0.6	1.17E-07	1.18E-07	1.18E-07	1.56E-01	1.57E-01	1.57E-01
0.5	0.5	0.5	9.76E-08	9.78E-08	9.81E-08	1.56E-01	1.56E-01	1.57E-01
0.4	0.4	0.4	7.81E-08	7.84E-08	7.87E-08	1.56E-01	1.57E-01	1.57E-01
0.3	0.3	0.3	5.82E-08	5.83E-08	5.85E-08	1.55E-01	1.55E-01	1.56E-01
0.2	0.2	0.2	3.83E-08	3.84E-08	3.86E-08	1.53E-01	1.53E-01	1.54E-01
0.1	0.1	0.1	1.81E-08	1.81E-08	1.81E-08	1.44E-01	1.45E-01	1.45E-01
0.05	0.05	0.05	7.87E-09	7.89E-09	7.61E-09	1.26E-01	1.26E-01	1.22E-01

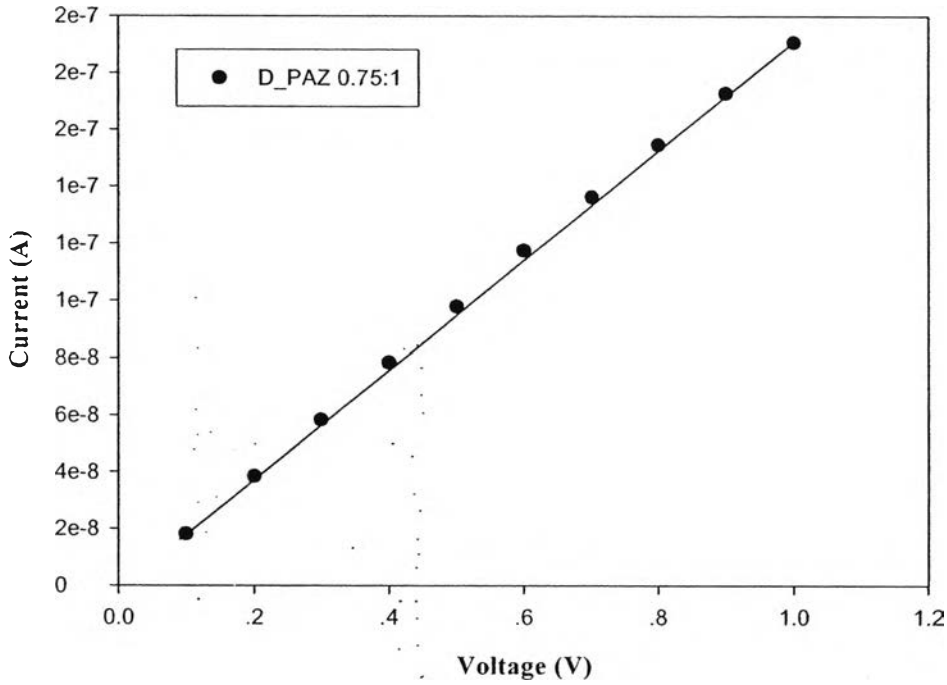

Figure B4 The Ohmic regime of D_PAZ 0.75:1 at thickness = 0.01942 cm, 25°C, 60-65 %RH.

Table B4 Voltage-current data in linear regime of D_PAZ 0.50:1 at 25°C, 60-65 %RH

Voltage (V)			Current (A)			Specific conductivity (S/cm)		
1	2	3	1	2	3	1	2	3
10	10	10	1.08E-07	1.08E-07	1.08E-07	8.87E-03	8.90E-03	8.87E-03
9	9	9	9.65E-08	9.63E-08	9.57E-08	8.85E-03	8.82E-03	8.77E-03
8	8	8	8.51E-08	8.47E-08	8.43E-08	8.77E-03	8.73E-03	8.69E-03
7	7	7	7.40E-08	7.41E-08	7.41E-08	8.71E-03	8.73E-03	8.73E-03
6	6	6	6.36E-08	6.39E-08	6.41E-08	8.75E-03	8.78E-03	8.81E-03
5	5	5	5.34E-08	5.34E-08	5.35E-08	8.80E-03	8.81E-03	8.83E-03
4	4	4	4.28E-08	4.27E-08	4.25E-08	8.82E-03	8.80E-03	8.76E-03
3	3	3	3.17E-08	3.17E-08	3.19E-08	8.73E-03	8.72E-03	8.78E-03
2	2	2	2.14E-08	2.14E-08	2.14E-08	8.82E-03	8.84E-03	8.84E-03
1	1	1	1.07E-08	1.06E-08	1.06E-08	8.79E-03	8.78E-03	8.77E-03
0.9	0.9	0.9	9.59E-09	9.63E-09	9.65E-09	8.79E-03	8.83E-03	8.84E-03
0.8	0.8	0.8	8.62E-09	8.66E-09	8.67E-09	8.88E-03	8.93E-03	8.94E-03
0.7	0.7	0.7	7.60E-09	7.59E-09	7.54E-09	8.96E-03	8.94E-03	8.88E-03
0.6	0.6	0.6	6.45E-09	6.48E-09	6.51E-09	8.86E-03	8.91E-03	8.95E-03
0.5	0.5	0.5	5.43E-09	5.44E-09	5.44E-09	8.96E-03	8.97E-03	8.98E-03
0.4	0.4	0.4	4.33E-09	4.33E-09	4.35E-09	8.93E-03	8.92E-03	8.96E-03
0.3	0.3	0.3	3.25E-09	3.25E-09	3.23E-09	8.93E-03	8.92E-03	8.89E-03

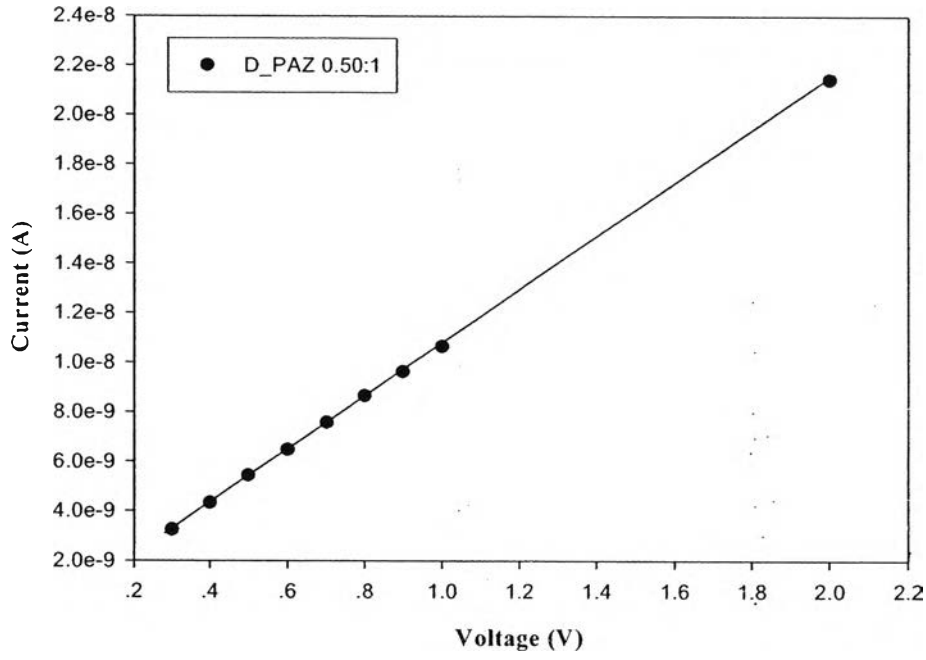

Figure B5 The Ohmic regime of D_PAZ 0.50:1 at thickness = 0.01883 cm, 25°C, 60-65 %RH.

Table B5 Voltage-current data in linear regime of D_PAZ 0.25:1 at 25°C, 60-65 %RH

Voltage (V)			Current (A)			Specific conductivity (S/cm)		
1	2	3	1	2	3	1	2	3
10	10	10	7.09E-09	6.95E-09	6.84E-09	8.00E-04	7.84E-04	7.72E-04
9	9	9	6.04E-09	5.97E-09	5.91E-09	7.58E-04	7.49E-04	7.41E-04
8	8	8	5.20E-09	5.14E-09	5.08E-09	7.34E-04	7.25E-04	7.16E-04
7	7	7	4.37E-09	4.33E-09	4.29E-09	7.05E-04	6.97E-04	6.91E-04
6	6	6	3.64E-09	3.61E-09	3.59E-09	6.85E-04	6.80E-04	6.75E-04
5	5	5	2.96E-09	2.95E-09	2.93E-09	6.69E-04	6.65E-04	6.61E-04
0.4	0.4	0.4	1.77E-09	1.77E-09	1.76E-09	4.99E-04	4.98E-04	4.95E-04
0.3	0.3	0.3	1.58E-10	1.57E-10	1.58E-10	5.94E-04	5.91E-04	5.94E-04
0.2	0.2	0.2	1.02E-10	1.02E-10	1.02E-10	5.74E-04	5.75E-04	5.76E-04
0.1	0.1	0.1	4.91E-11	4.92E-11	4.93E-11	5.55E-04	5.56E-04	5.56E-04
0.09	0.09	0.09	3.82E-11	3.84E-11	3.83E-11	4.79E-04	4.82E-04	4.81E-04
0.08	0.08	0.08	2.68E-11	2.68E-11	2.68E-11	3.78E-04	3.79E-04	3.79E-04
0.07	0.07	0.07	1.74E-11	1.74E-11	1.75E-11	2.80E-04	2.81E-04	2.83E-04
0.06	0.06	0.06	1.52E-11	1.52E-11	1.49E-11	2.86E-04	2.86E-04	2.81E-04
0.05	0.05	0.05	1.17E-11	1.16E-11	1.15E-11	2.65E-04	2.63E-04	2.60E-04
0.04	0.04	0.04	8.84E-12	8.66E-12	8.74E-12	2.49E-04	2.44E-04	2.46E-04
0.03	0.03	0.03	5.96E-12	5.96E-12	5.84E-12	2.24E-04	2.24E-04	2.20E-04
0.02	0.02	0.02	3.47E-12	3.50E-12	3.52E-12	1.96E-04	1.97E-04	1.98E-04
0.01	0.01	0.01	2.09E-12	2.11E-12	2.13E-12	2.36E-04	2.38E-04	2.40E-04

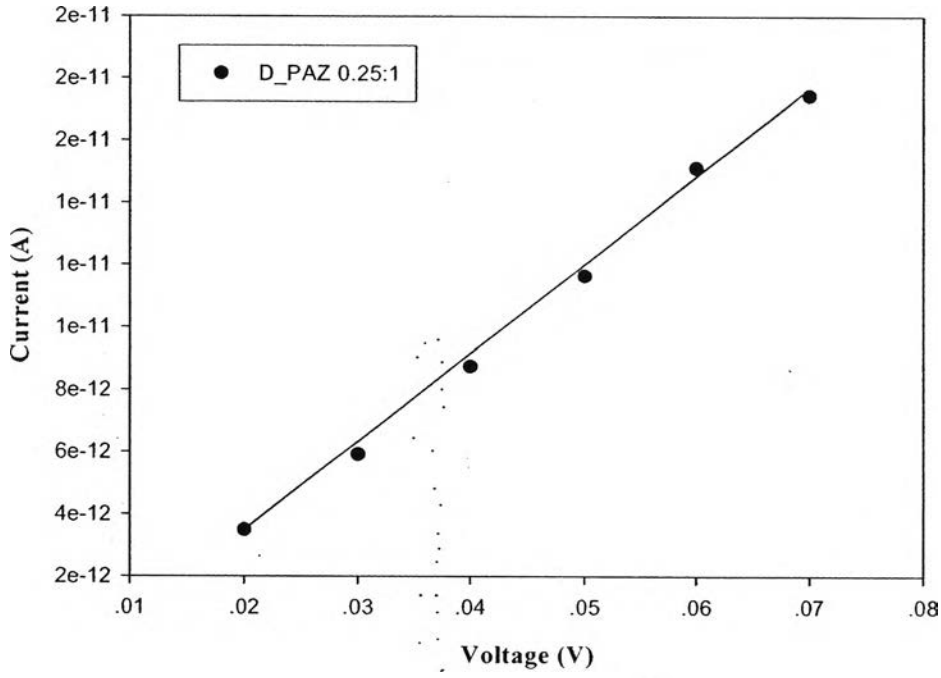

Figure B6 The Ohmic regime of D_PAZ 0.25:1 at thickness = 0.01376 cm, 25˚C, 60-65 %RH.

Appendix C Density Determination by Pycnometer

The density of dedoped-Permethylpolyazine and the doped-polymers with various doping mole ratios was determined by using Pycnometer with a small cell size. The polymers were firstly vacuum-dried for 24 hr and then weighted at ambient temperature, loaded the sample to the cell. Density determination was carried out 3 time for each sample.

Table C1 Density data of dedoped-permethylpolyazine (De_PAZ) measured at 27 °C.

Run	**Volume (cm^3)**	**Density (g/cm^3)**
1	0.1316	0.7120
2	0.1770	0.7977
3	0.2186	0.8230

Average Volume	0.175733 cm^3
Average Density	0.777567 g/cm^3
Standard Deviation	0.058174 g/cm^3

Table C2 Density data of doped-permethylpolyazine (D_PAZ) at doping mole ratio N_{iodine}:$N_{monomer}$, 0.25:1 (D_PAZ 0.25:1) measured at 27 °C.

Run	Volume (cm^3)	Density (g/cm^3)
1	0.1710	1.2156
2	0.1996	1.2320
3	0.2671	1.2460

Average Volume	0.212567 cm^3
Average Density	1.2312 g/cm^3
Standard Deviation	0.015216 g/cm^3

Table C3 Density data of doped-permethylpolyazine (D_PAZ) at doping mole ratio N_{iodine}:$N_{monomer}$, 0.50:1 (D_PAZ 0.50:1) measured at 27 °C.

Run	Volume (cm^3)	Density (g/cm^3)
1	0.1660	1.737
2	0.0820	1.781
3	0.1671	1.735

Average Volume	0.138367 cm^3
Average Density	1.751 g/cm^3
Standard Deviation	0.026 g/cm^3

Table C4 Density data of doped-permethylpolyazine (D_PAZ) at doping mole ratio N_{iodine}:$N_{monomer}$, 0.75:1 (D_PAZ 0.75:1) measured at 27 °C.

Run	Volume (cm^3)	Density (g/cm^3)
1	0.3343	1.810
2	0.3243	1.960
3	0.3244	1.791

Average Volume	0.327667 cm^3
Average Density	1.862333 g/cm^3
Standard Deviation	0.084654 g/cm^3

Table C5 Density data of doped-permethylpolyazine (D_PAZ) at doping mole ratio N_{iodine}:$N_{monomer}$, 1.00:1 (D_PAZ 1.00:1) measured at 27 °C.

Run	Volume (cm^3)	Density (g/cm^3)
1	0.3243	1.805
2	0.3443	1.831
3	0.2844	1.764

Average Volume	0.317667 cm^3
Average Density	1.8 g/cm^3
Standard Deviation	0.033779 g/cm^3

Appendix D Electromechanical Properties Measurement of EPDM with different ENB contents

Strain Sweep Test: pure EPDM film by using parallel plates

The temporal response of pure EPDM films with different ENB content; NORDEL IP 3670; NORDEL IP 4570; and NORDEL IP 5565 were carried out by melt rheometer meter (Rheometric Scientific, ARES). It was fitted with a custom-built copper parallel plates fixture, diameter 25 mm. A DC voltage was applied by DC power supply (Instek, GFG 8216A), which can deliver electric field strength to 2 kV/mm. A digital multimeter was used to monitor the voltage input. For temporal responses testing, oscillate shear strain was applied and the dynamic moduli (G' and G") were investigated as a function of time and electric field strength. Dynamic strain sweep test were first carried out to determine appropriate strains by measured G′ and G″ in linear viscoelastic regime. The following figures, Figure D1, D2, and D3, show linear viscoelastic regimes of pure EPDM films: NORDEL IP 3670; NORDEL IP 4570; and NORDEL IP 5565, respectively, without electric field strength (0 V/mm). Besides, Figure D4, D5, and D6, show the linear viscoelastic regimes of pure EPDM films in the influence of electric field strength at 1 kV/mm.

Table D1 Storage modulus and loss modulus data, obtained from dynamic strain sweep test of NORDEL IP 3670 (1.8% of ENB), parallel plate, gap = 0.676 mm, film diameter = 25 mm, electric field (E) = 0 V/mm, 27°C

%Strain	G' (Pa)	G" (Pa)	%Strain	G' (Pa)	G" (Pa)
0.02549	80529.5	7006.29	1.6789	1.00E+05	19577.8
0.04187	86179.8	5650.92	2.6634	1.00E+05	22158
0.06712	86623.5	7493.78	4.23617	97379.9	24458.3
0.10611	90395.9	9625.85	6.754	86768.9	24038.4
0.16851	90689.1	11469.5	10.775	80856.8	24763.2
0.26746	91398.9	11962.8	17.1971	75670.2	23263.2
0.42072	95025.3	13376.4	27.5691	67838.8	29409.5
0.66484	97818.1	16450.4	43.2825	74549.7	27731.4
1.05907	99298.3	17817.7			

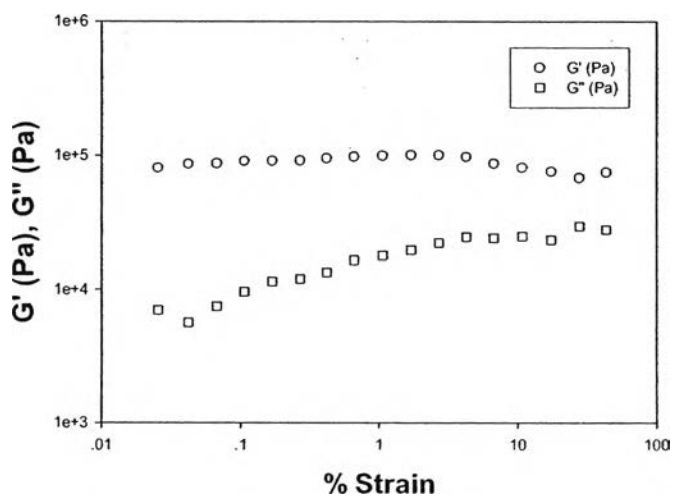

Figure D1 Storage modulus and loss modulus versus strain (%) obtained from dynamic strain sweep test of NORDEL IP 3670 (1.8% of ENB), parallel plate, gap = 0.676 mm, film diameter = 25 mm, electric field (E) = 0 V/mm, 27°C.

Table D2 Storage modulus and loss modulus data, obtained from dynamic strain sweep test of NORDEL IP 4570 (4.9% of ENB), parallel plate, gap = 0.638 mm, film diameter = 25 mm, electric field (E) = 0 V/mm, 27°C

%Strain	G' (Pa)	G" (Pa)	%Strain	G' (Pa)	G" (Pa)
0.02578	75658.8	25403.8	1.74301	66360.2	21452.8
0.04135	82177.9	26847.8	2.77253	63987.1	20271
0.06685	79412.9	25941.5	4.40059	62870.8	19266.9
0.10633	80351.8	22089.6	6.9847	61979.4	19746.2
0.16879	79628	22989.6	11.1537	53424.2	18992.3
0.26991	77982.9	22251.9	17.7426	49776.9	18762
0.42861	75659	22122.2	28.131	49848.6	21526.3
0.68263	73969.4	21578	45.2572	37811.7	21268.5
1.09406	70335.6	22102.2			

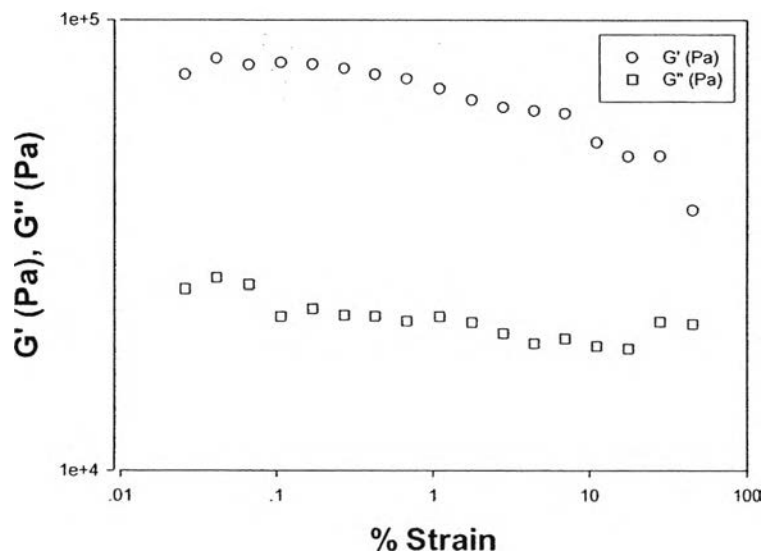

Figure D2 Storage modulus and loss modulus versus strain (%) obtained from dynamic strain sweep test of NORDEL IP 4570 (4.9% of ENB), parallel plate, gap = 0.638 mm, film diameter = 25 mm, electric field (E) = 0 V/mm, 27°C.

Table D3 Storage modulus and loss modulus data, obtained from dynamic strain sweep test of NORDEL IP 5565 (7.5% of ENB), parallel plate, gap = 0.464 mm, film diameter = 25 mm, electric field (E) = 0 V/mm, 27°C

%Strain	G' (Pa)	G" (Pa)	%Strain	G' (Pa)	G" (Pa)
0.0239	1.32E+05	27319.7	1.55063	1.20E+05	34619.6
0.0371	1.23E+05	34169.5	2.46047	1.19E+05	34551.1
0.06117	1.23E+05	30896.5	3.90261	1.19E+05	34992.9
0.09601	1.26E+05	38561.2	6.19617	1.11E+05	32974.2
0.15286	1.24E+05	36914.1	9.85835	1.09E+05	33375.1
0.24282	1.23E+05	34896.2	16.7946	64406.6	43999
0.38523	1.23E+05	35217.2	27.2526	51587.6	34208.1
0.61126	1.22E+05	35067.6	43.0272	54197.8	27362.2
0.96873	1.21E+05	34860.1			

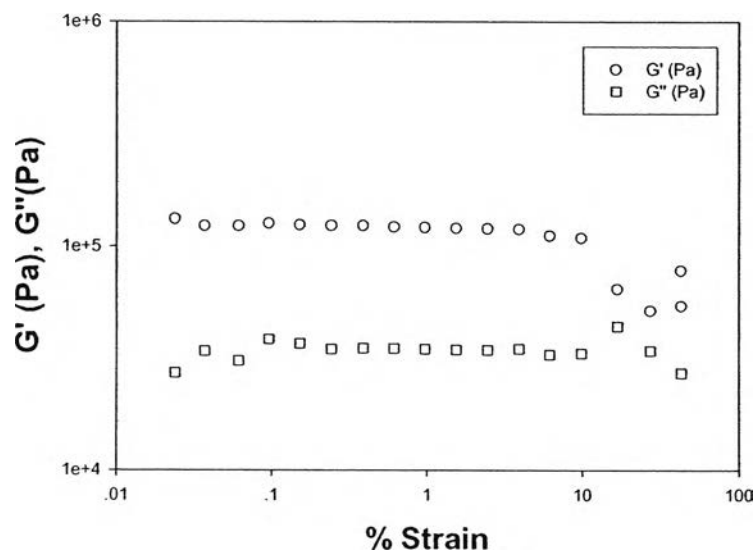

Figure D3 Storage modulus and loss modulus versus strain (%) obtained from dynamic strain sweep test of NORDEL IP 5565 (7.5% of ENB), parallel plate, gap = 0.464 mm, film diameter = 25 mm, electric field (E) = 0 V/mm, 27°C.

Table D4 Storage modulus and loss modulus data, obtained from dynamic strain sweep test of NORDEL IP 3670 (1.8% of ENB), parallel plate, gap = 0.676 mm, film diameter = 25 mm, electric field (E) = 1 V/mm, 27°C

%Strain	G' (Pa)	G" (Pa)	%Strain	G' (Pa)	G" (Pa)
0.0263	70913.5	11063.4	1.72319	73391.9	20354.3
0.04215	76223.7	21337	2.7337	72987.9	20865.4
0.06726	74956.8	21525.4	4.34209	71558.9	21510.9
0.10738	74980.5	20659.9	6.92192	66601.4	22552.8
0.17161	74311.5	20426.5	11.1214	52515.3	20925.8
0.27133	74429.4	20356.8	17.7997	45420.5	19972.2
0.43067	74003	20448.9	28.4094	40304.6	17291.3
0.68183	74047.1	20489.5	45.7588	28104.8	12385.3
1.0857	73852.4	20335.3			

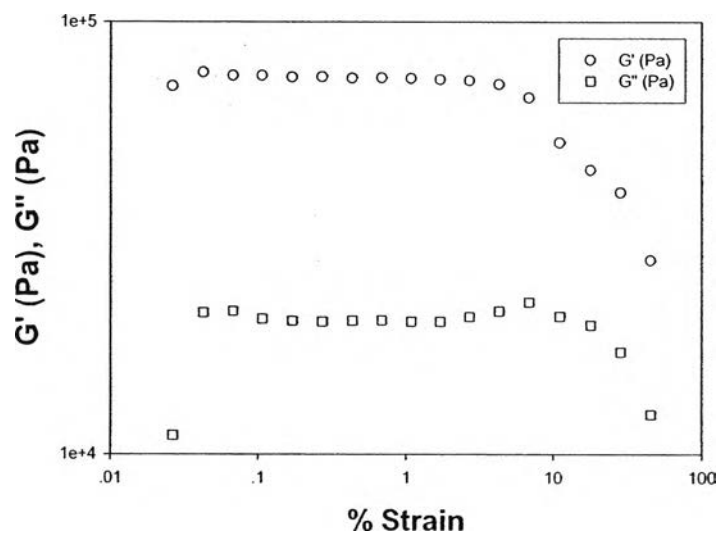

Figure D4 Storage modulus and loss modulus versus strain (%) obtained from dynamic strain sweep test of NORDEL IP 3670 (1.8% of ENB), parallel plate, gap = 0.676 mm, film diameter = 25 mm, electric field (E) = 1 V/mm, 27°C.

Table D5 Storage modulus and loss modulus data, obtained from dynamic strain sweep test of NORDEL IP 4570 (4.9% of ENB), parallel plate, gap = 0.638 mm, film diameter = 25 mm, electric field (E) = 1 V/mm, 27°C

%Strain	G' (Pa)	G" (Pa)	%Strain	G' (Pa)	G" (Pa)
0.02435	1.70E+05	28083.9	1.46229	1.84E+05	58476.3
0.03715	1.90E+05	24737.5	2.37195	1.66E+05	55128.6
0.05828	1.92E+05	28535.2	4.10754	95937.9	77880.1
0.09188	1.96E+05	30344.1	6.95005	50512.9	60339.1
0.14225	2.17E+05	31136.2	11.4145	27633.5	41687.4
0.21613	2.44E+05	34552.5	18.2968	19969.8	24802.6
0.33355	2.67E+05	46303.4	27.8453	46222.6	15977.2
0.52399	2.71E+05	59741.4	42.1227	77778.1	23065.8
0.87463	2.30E+05	64502.6			

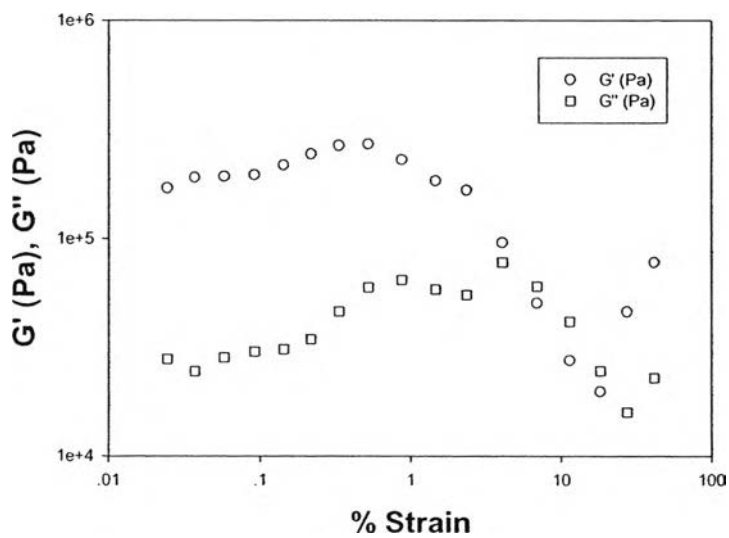

Figure D5 Storage modulus and loss modulus versus strain (%) obtained from dynamic strain sweep test of NORDEL IP 4570 (4.9% of ENB), parallel plate, gap = 0.638 mm, film diameter = 25 mm, electric field (E) = 1 V/mm, 27°C.

Table D6 Storage modulus and loss modulus data, obtained from dynamic strain sweep test of NORDEL IP 5565 (7.5% of ENB), parallel plate, gap = 0.464 mm, film diameter = 25 mm, electric field (E) = 1 V/mm, 27°C

%Strain	G' (Pa)	G" (Pa)	%Strain	G' (Pa)	G" (Pa)
0.02379	1.46E+05	40839.5	1.49244	1.45E+05	41662.5
0.03513	1.59E+05	37850.9	2.37007	1.45E+05	42037.6
0.05673	1.53E+05	47163	3.75927	1.44E+05	41919.1
0.09294	1.49E+05	40048.3	5.97055	1.35E+05	39598.2
0.14682	1.50E+05	42817.7	9.48991	1.33E+05	39786.8
0.23303	1.51E+05	42123.4	16.653	68956.4	49588.8
0.37159	1.48E+05	42977.8	26.9457	57886.2	38723.3
0.58828	1.47E+05	42943.9	42.2851	65315.6	31890.2
0.93394	1.46E+05	41762.3			

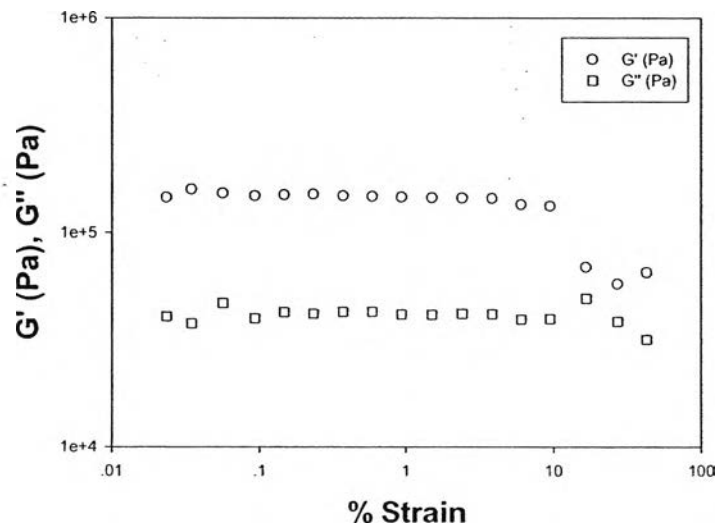

Figure D6 Storage modulus and loss modulus versus strain (%) obtained from dynamic strain sweep test of NORDEL IP 5565 (7.5% of ENB), parallel plate, gap = 0.464 mm, film diameter = 25 mm, electric field (E) = 1 V/mm, 27°C.

Time Sweep Test: pure EPDM film by using parallel plates

The time sweep test was carried out with electric field applied on and off, alternately. The G'of each film was investigated to measure until each film response reaches a steady state and to find whether the response under electric field stimulation is irreversible or not. Because they are low dielectric materials. Thus, the force generated under electric field is low. The effective actuation force is given by (Pelrine *et al., 2000*):

$$p = \varepsilon\varepsilon_0 E^2 = \varepsilon\varepsilon_0 (V/z)^2 \qquad \text{(D.1)}$$

where p is the actuation pressure, E is the electric field strength, ε is the dielectric constant, ε_0 is the permittivity of free space, V is voltage, and z is the polymer thickness.

The time sweep test of NORDEL IP 3670 (1.8% of ENB) are shown in Figure D7 and D8 reversed film to another surface, heated it up and cooled it down, respectively was carried out with electric field applied on and off, alternately. The G'of this film was investigated to measure the time each film response reaches a steady state and there is response under electric field stimulation but irreversible.

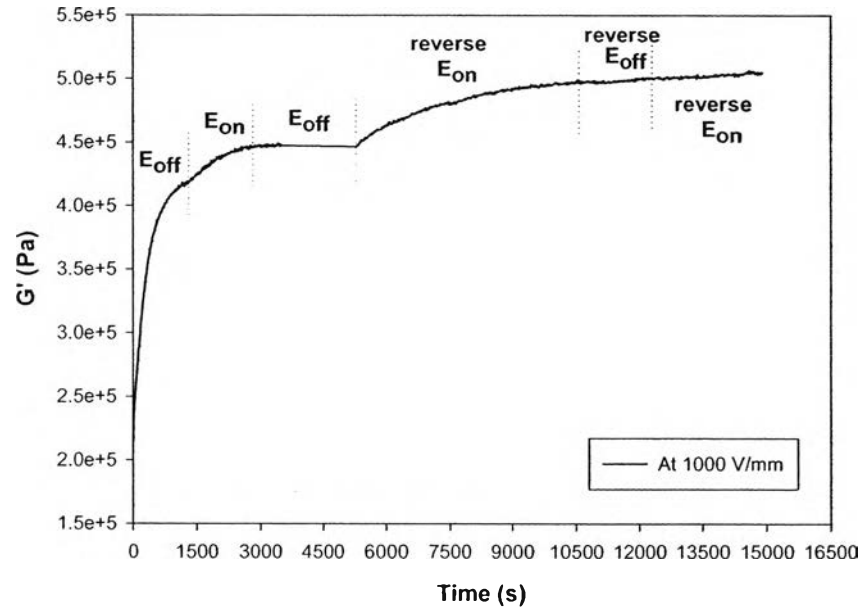

Figure D7 Temporal response testing of storage modulus (G′) of NORDEL IP 3670 (1.8% of ENB), parallel plate, strain 0.2 %, gap 0.601 mm, film diameter 25 mm, frequency 100 rad/s, electric field (E) 1 kV/mm, 27°C.

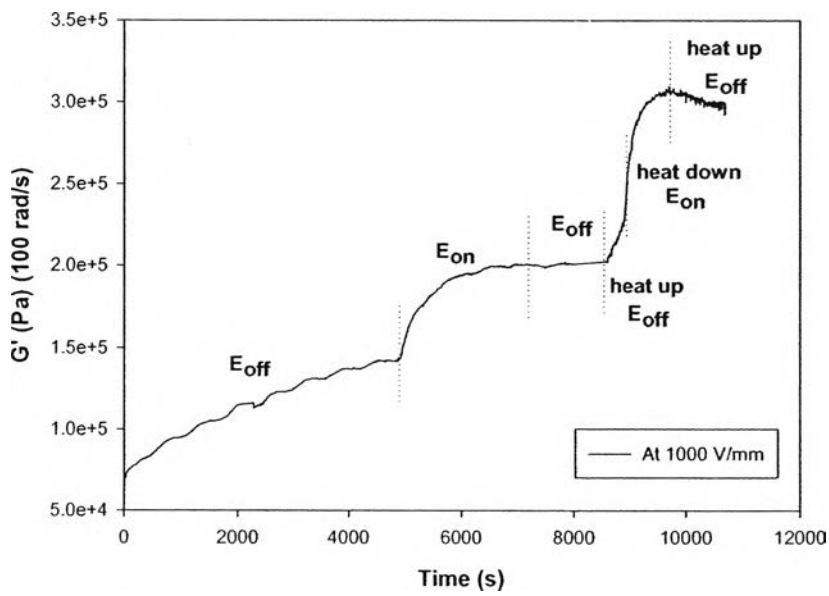

Figure D8 Temporal response testing of storage modulus (G′) of NORDEL IP 3670 (1.8% of ENB), parallel plate, strain 0.2 %, gap 0.854 mm, film diameter 25 mm, frequency 100 rad/s, electric field (E) 1 kV/mm, 27°C.

Appendix E Frequency Sweep Test of pure EPDM films with different ENB contents; various electric fields.

Frequency test of NORDEL IP 3670 (1.8% of ENB)

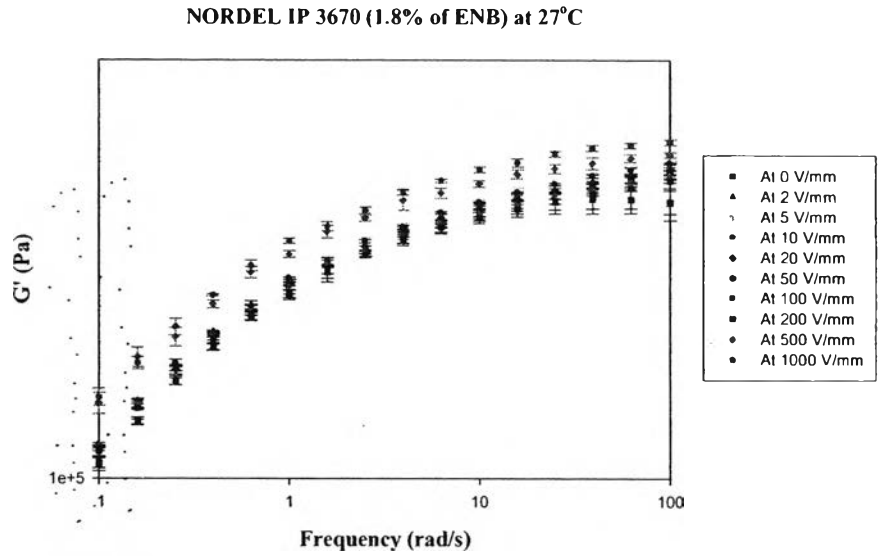

Figure E1 NORDEL IP 3670 at T = 27°C, strain 0.2 % frequency sweep test at various electric field strength (V/mm).

The storage modulus response of NORDEL IP 3670 (1.8% of ENB)

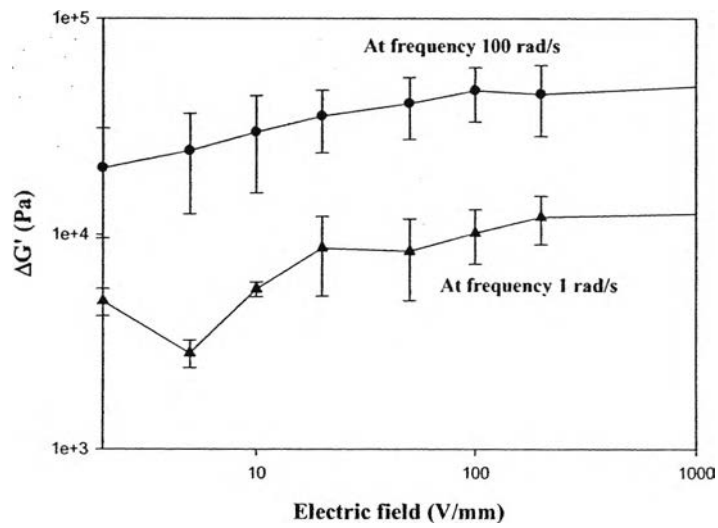

Figure E2 The storage modulus response (ΔG') at T=27°C, and %strain=0.2, vs. electric field strength (V/mm) of NORDEL IP 3670.

The sensitivity of the storage modulus of NORDEL IP 3670 (1.8% of ENB)

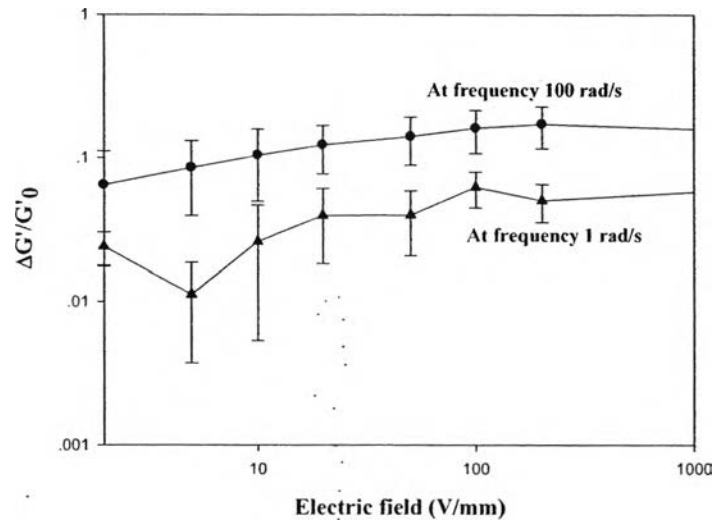

Figure E3 The sensitivity of the storage modulus □ΔG'/G'$_0$) at T=27°C, and %strain=0.2, vs. electric field strength (V/mm) of NORDEL IP 3670 (G'$_{0\ \text{at frequency 1.0 rad/s}}$=205,265 Pa and G'$_{0\ \text{at frequency 100 rad/s}}$=297,555 Pa.

Frequency test of NORDEL IP 4570 (4.9% of ENB)

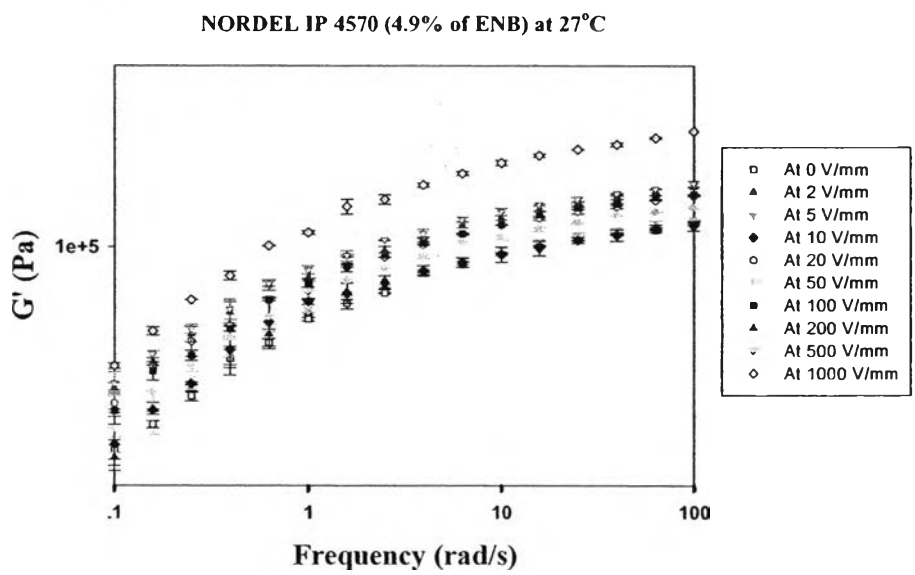

Figure E4 NORDEL IP 4570 at T = 27°C, strain 0.06 % frequency sweep test at various electric field strength (V/mm).

The storage modulus response of NORDEL IP 4570 (4.9% of ENB)

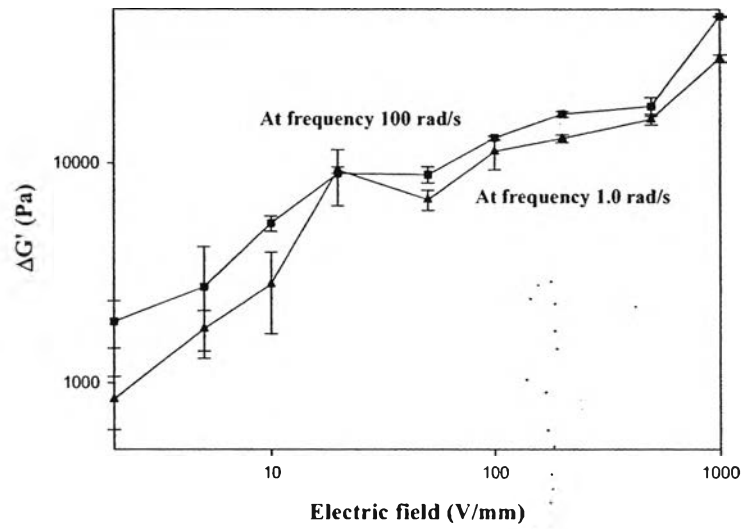

Figure E5 The storage modulus response (□ΔG') at T=27°C, and %strain=0.06, vs. electric field strength (V/mm) of NORDEL IP 4570.

The sensitivity of the storage modulus of NORDEL IP 4570 (4.9% of ENB

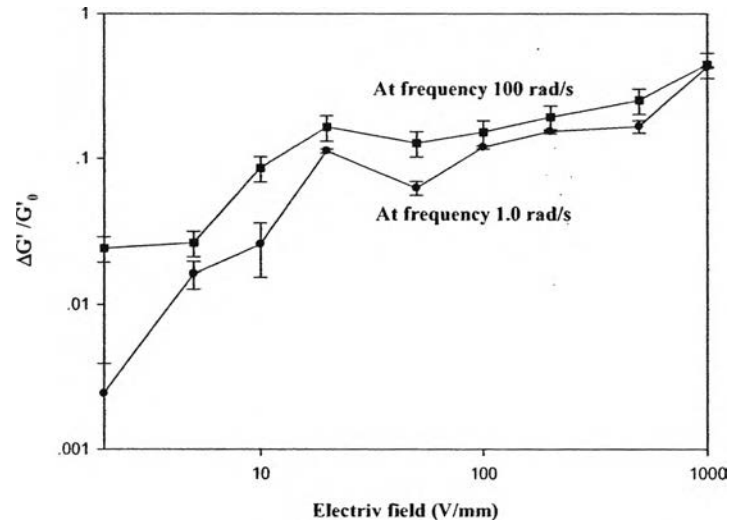

Figure E6 The sensitivity of the storage modulus □($\Delta G'/G'_0$) at T=27°C, and %strain=0.06, vs. electric field strength (V/mm) of NORDEL IP 4570 ($G'_{0\ \text{at frequency 1.0 rad/s}}$=75,726.7 Pa and $G'_{0\ \text{at frequency 100 rad/s}}$=109,220 Pa).

Frequency test of NORDEL IP 5565 (7.5% of ENB)

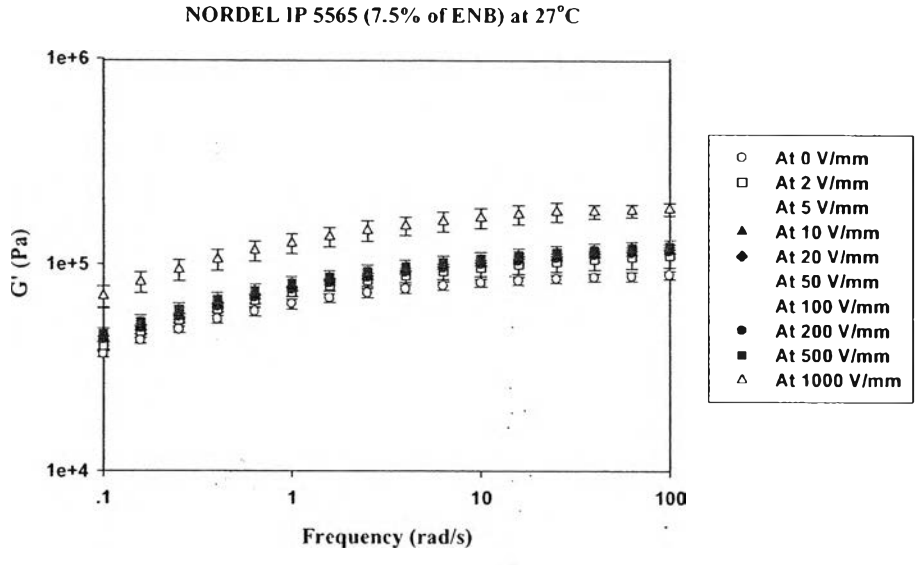

Figure E7 NORDEL IP 5565 at T = 27°C, strain 0.3 % frequency sweep test at various electric field strength (V/mm).

The storage modulus response of NORDEL IP 5565 (7.5% of ENB)

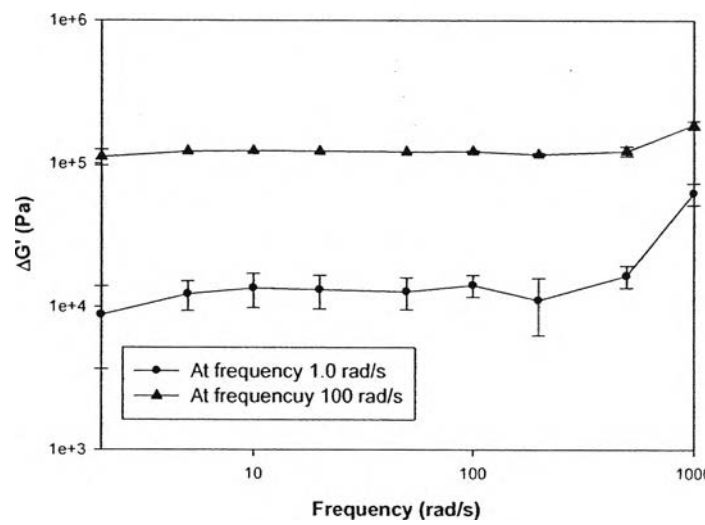

Figure E8 The storage modulus response □(ΔG') at T=27°C, and %strain=0.3, vs. electric field strength (V/mm) of NORDEL IP 5565.

The sensitivity of the storage modulus of NORDEL IP 5565 (7.5% of ENB)

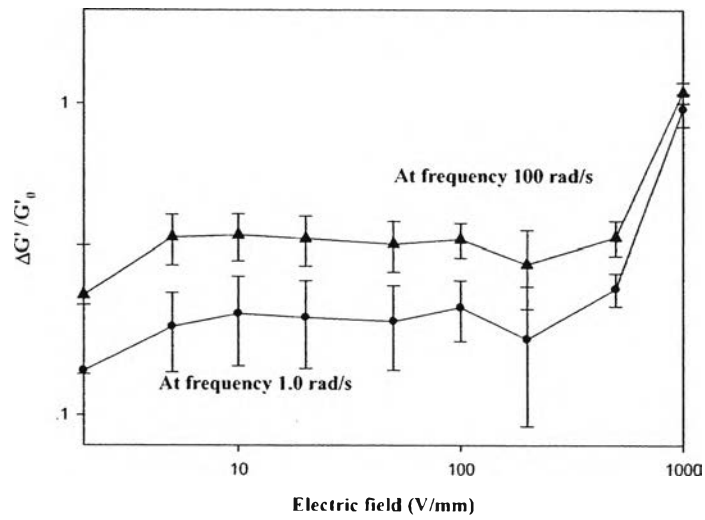

Figure E9 The sensitivity of the storage modulus □ΔG'/G'$_0$) at T=27°C, and %strain=0.3, vs. electric field strength (V/mm) of NORDEL IP 5565 (G'$_{0\ \text{at frequency 1.0 rad/s}}$=26,725 Pa and G'$_{0\ \text{at frequency 100 rad/s}}$=91,248.75 Pa).

Appendix F Electrorheological Properties Measurement of EPDM with molecular weight contents

Strain Sweep Test: pure EPDM film by using parallel plates

The temporal response of pure EPDM films with different molecular weight content; NORDEL IP 4520; NORDEL IP 4640; and NORDEL IP 4570 were carried out by melt rheometer meter (Rheometric Scientific, ARES). It was fitted with a custom-built copper parallel plates fixture, diameter 25 mm. A DC voltage was applied by DC power supply (Instek, GFG 8216A), which can deliver electric field strength to 2 kV/mm. A digital multimeter was used to monitor the voltage input. For temporal responses testing, oscillate shear strain was applied and the dynamic moduli (G' and G") were investigated as a function of time and electric field strength. Dynamic strain sweep test were first carried out to determine appropriate strains by measured G' and G" in linear viscoelastic regime. The following figures, Figure F1, F2, and F3, show linear viscoelastic regimes of pure EPDM films: NORDEL IP 4520; NORDEL IP 4640; and NORDEL IP 4570, respectively, without electric field strength (0 V/mm). Besides, Figure F4, F5, and F6, show the linear viscoelastic regimes of pure SIS films in the influence of electric field strength at 1 kV/mm.

Table F1 Storage modulus and loss modulus data, obtained from dynamic strain sweep test of NORDEL IP 4520 (MW=115,000), parallel plate, gap = 0.567 mm, film diameter = 25 mm, electric field (E) = 0 V/mm, 27°C

%Strain	G' (Pa)	G" (Pa)	%Strain	G' (Pa)	G" (Pa)
0.02687	98311.1	29716.9	1.60536	1.18E+05	55113.6
0.04115	1.04E+05	39923.7	2.52532	1.24E+05	56281.2
0.06612	94804.6	37693.2	3.98892	1.26E+05	59698.1
0.10315	1.05E+05	43097.3	6.39665	1.10E+05	62510
0.15967	1.14E+05	44866.5	10.7383	69474.8	56051.5
0.25092	1.14E+05	51362.7	17.4602	52507.8	42500.2
0.39985	1.15E+05	51469.3	28.0563	43073.1	31983.4
0.63346	1.16E+05	52960.5	43.4183	60179	27967.1
1.01648	1.15E+05	53495.9			

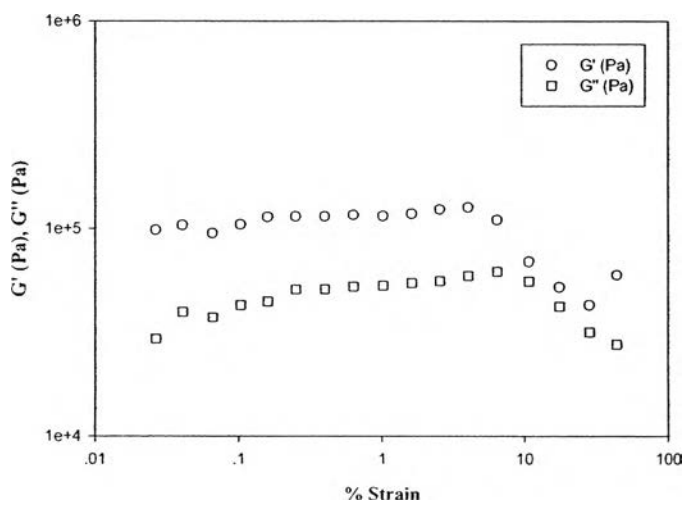

Figure F1 Storage modulus and loss modulus versus strain (%) obtained from dynamic strain sweep test of NORDEL IP 4520 (MW=115,000), parallel plate, gap = 0.567 mm, film diameter = 25 mm, electric field (E) = 0 V/mm, 27°C.

Table F2 Storage modulus and loss modulus data, obtained from dynamic strain sweep test of NORDEL IP 4640 (MW=160,000), parallel plate, gap = 0.538 mm, film diameter = 25 mm, electric field (E) = 0 V/mm, 27°C

%Strain	G' (Pa)	G" (Pa)	%Strain	G' (Pa)	G" (Pa)
0.0264	21239.7	5467.41	1.8294	19995.8	5851.32
0.0439	21313.9	6508.91	2.9065	19110.6	6062.31
0.0704	19198.2	4647.22	4.6347	15580.8	7148.62
0.1131	19432.4	4604.33	7.4229	8653.27	7063.83
0.1803	19114	4340.83	11.8368	5731.02	5127.68
0.2877	19049.5	4979.22	18.7499	5963.15	3818.33
0.4563	19608.4	4813.85	29.7189	5753.03	3171.39
0.7232	20468.8	5043.04	47.0638	7457.45	3066.07
1.1549	20579.3	5561.94			

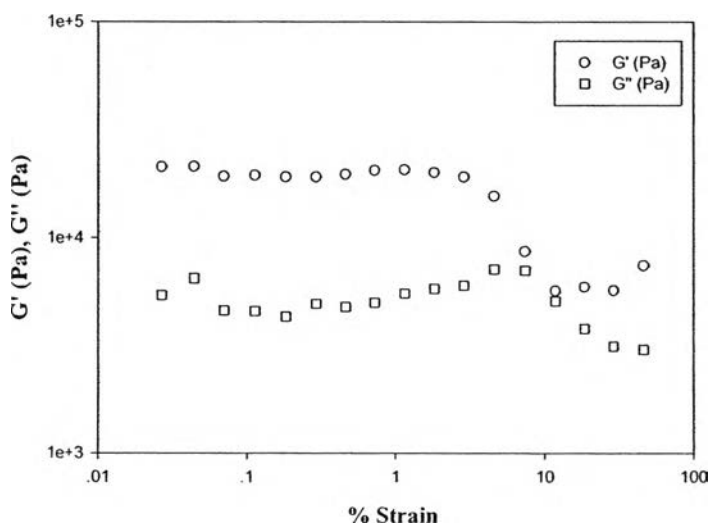

Figure F2 Storage modulus and loss modulus versus strain (%) obtained from dynamic strain sweep test of NORDEL IP 4640 (MW=160,000), parallel plate, gap = 0.538 mm, film diameter = 25 mm, electric field (E) = 0 V/mm, 27°C.

Table F3 Storage modulus and loss modulus data, obtained from dynamic strain sweep test of NORDEL IP 4570 (MW=210,000), parallel plate, gap = 0.638 mm, film diameter = 25 mm, electric field (E) = 0 V/mm, 27°C

%Strain	G' (Pa)	G" (Pa)	%Strain	G' (Pa)	G" (Pa)
0.02578	75658.8	25403.8	1.74301	66360.2	21452.8
0.04135	82177.9	26847.8	2.77253	63987.1	20271
0.06685	79412.9	25941.5	4.40059	62870.8	19266.9
0.10633	80351.8	22089.6	6.9847	61979.4	19746.2
0.16879	79628	22989.6	11.1537	53424.2	18992.3
0.26991	77982.9	22251.9	17.7426	49776.9	18762
0.42861	75659	22122.2	28.131	49848.6	21526.3
0.68263	73969.4	21578	45.2572	37811.7	21268.5
1.09406	70335.6	22102.2			

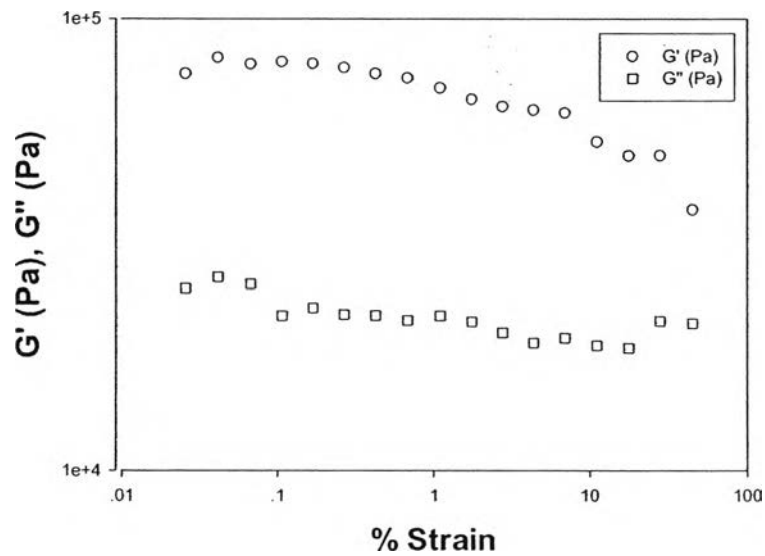

Figure F3 Storage modulus and loss modulus versus strain (%) obtained from dynamic strain sweep test of NORDEL IP 4570 (MW=210,000), parallel plate, gap = 0.638 mm, film diameter = 25 mm, electric field (E) = 0 V/mm, 27°C.

Table F4 Storage modulus and loss modulus data, obtained from dynamic strain sweep test of NORDEL IP 4520 (MW=115,000), parallel plate, gap = 0.567 mm, film diameter = 25 mm, electric field (E) = 1 V/mm, 27°C

%Strain	G' (Pa)	G" (Pa)	%Strain	G' (Pa)	G" (Pa)
0.0236	1.26E+05	61628.3	1.55683	1.41E+05	74103
0.03966	1.27E+05	59907.7	2.46464	1.42E+05	74815.7
0.06075	1.37E+05	69773.1	3.90459	1.43E+05	75327.6
0.09712	1.38E+05	68118.5	6.28767	1.23E+05	74854.8
0.1541	1.37E+05	69598.9	10.7127	69943.4	64702.3
0.24253	1.39E+05	71664.1	17.3815	54446.6	48008.8
0.38662	1.39E+05	72479.3	27.9689	45022.1	34903.9
0.61461	1.40E+05	73693.4	43.0074	66695	31296.7
0.98249	1.41E+05	73729.5			

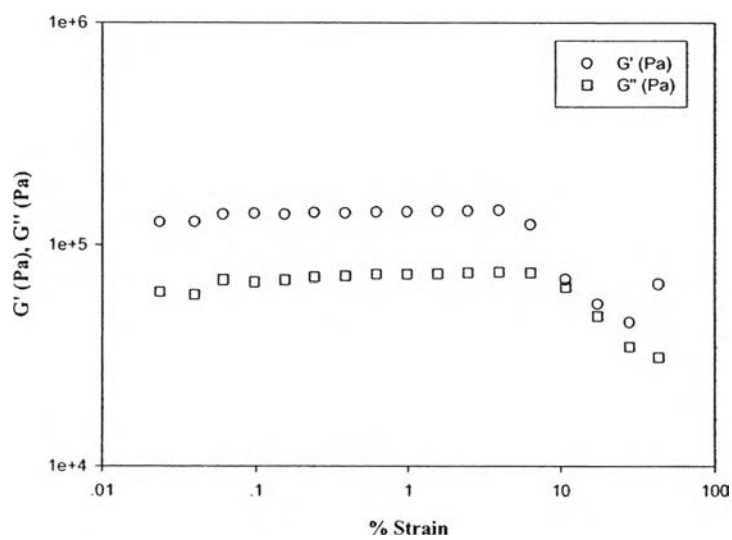

Figure F4 Storage modulus and loss modulus versus strain (%) obtained from dynamic strain sweep test of NORDEL IP 4520 (MW=115,000), parallel plate, gap = 0.567 mm, film diameter = 25 mm, electric field (E) = 1 V/mm, 27°C.

Table F5 Storage modulus and loss modulus data, obtained from dynamic strain sweep test of NORDEL IP 4640 (MW=160,000), parallel plate, gap = 0.538 mm, film diameter = 25 mm, electric field (E) = 1 V/mm, 27°C

%Strain	G' (Pa)	G" (Pa)	%Strain	G' (Pa)	G" (Pa)
0.0314	21105.7	5609.19	1.8362	18268.4	7751.43
0.0454	22293.2	6627.73	2.9331	12863.9	8472.02
0.0697	23597.9	7210.45	4.6948	7031.61	7241.43
0.1127	22259.9	7220.16	7.4805	3762.35	5260.26
0.1797	22264.2	7008.59	11.8932	2148.74	3683.24
0.2856	22192.7	6595.85	18.8296	3405.63	2778.76
0.4523	22888.4	7238.1	29.6881	6351.78	2688.42
0.717	23804.4	7509.92	46.9042	8372.01	3188.52
1.1497	22108.4	7424.37			

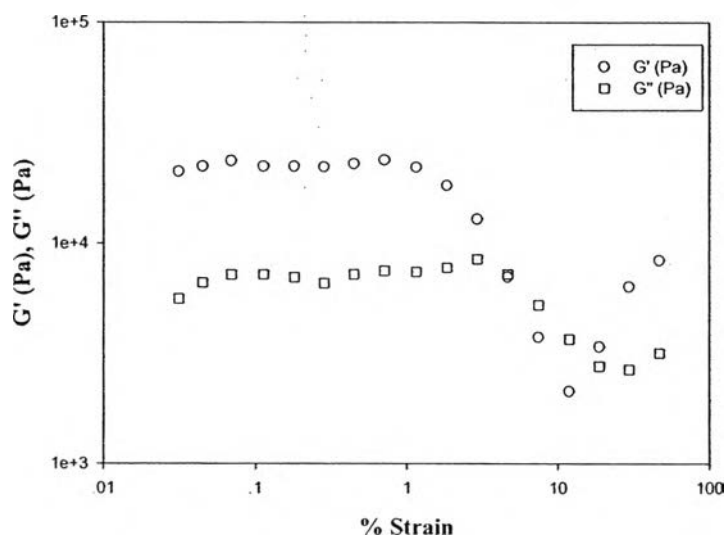

Figure F5 Storage modulus and loss modulus versus strain (%) obtained from dynamic strain sweep test of NORDEL IP 4640 (MW=160,000), parallel plate, gap = 0.538 mm, film diameter = 25 mm, electric field (E) = 1 V/mm, 27°C.

Table F6 Storage modulus and loss modulus data, obtained from dynamic strain sweep test of NORDEL IP 4570 (MW=210,000), parallel plate, gap = 0.638 mm, film diameter = 25 mm, electric field (E) = 1 V/mm, 27°C

%Strain	G' (Pa)	G" (Pa)	%Strain	G' (Pa)	G" (Pa)
0.02435	1.70E+05	28083.9	1.46229	1.84E+05	58476.3
0.03715	1.90E+05	24737.5	2.37195	1.66E+05	55128.6
0.05828	1.92E+05	28535.2	4.10754	95937.9	77880.1
0.09188	1.96E+05	30344.1	6.95005	50512.9	60339.1
0.14225	2.17E+05	31136.2	11.4145	27633.5	41687.4
0.21613	2.44E+05	34552.5	18.2968	19969.8	24802.6
0.33355	2.67E+05	46303.4	27.8453	46222.6	15977.2
0.52399	2.71E+05	59741.4	42.1227	77778.1	23065.8
0.87463	2.30E+05	64502.6			

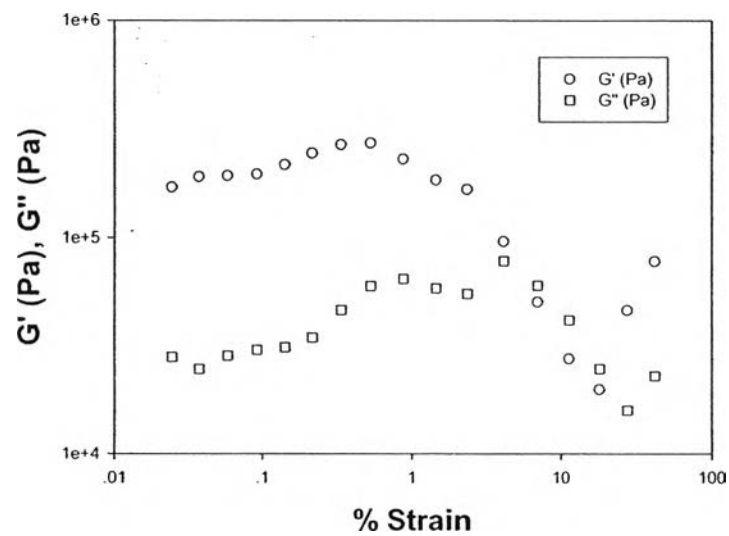

Figure F6 Storage modulus and loss modulus versus strain (%) obtained from dynamic strain sweep test of NORDEL IP 4570 (MW=210,000), parallel plate, gap = 0.638 mm, film diameter = 25 mm, electric field (E) = 1 V/mm, 27°C.

Appendix G Frequency Sweep Test of pure EPDM films with different molecular weight contents; various electric fields.

Frequency test of NORDEL IP 4520 (M_W=115,000)

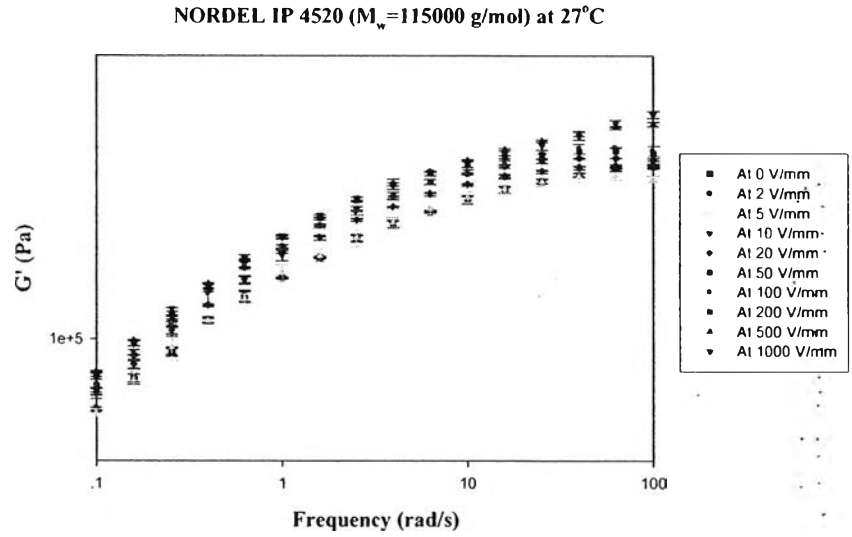

Figure G1 NORDEL IP 4520 at T = 27°C, strain 0.2 % frequency sweep test at various electric field strength (V/mm).

The storage modulus response of NORDEL IP 4520 (M_W=115,000)

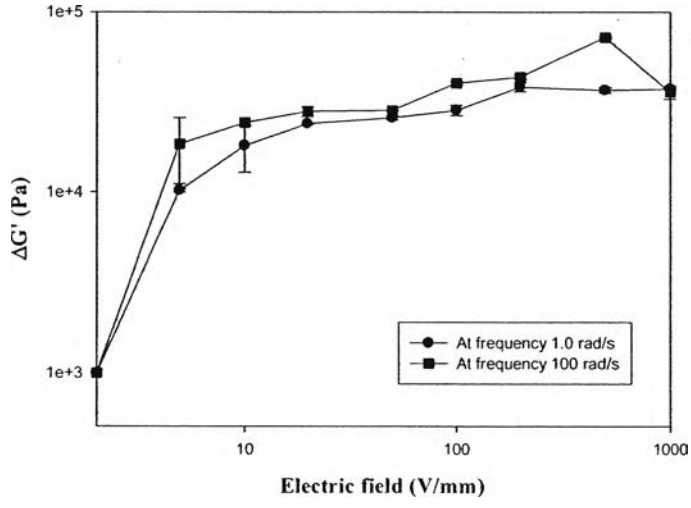

Figure G2 The storage modulus response □(ΔG') at T = 27°C, strain 0.2 %, vs. electric field strength (V/mm) of NORDEL IP 4520.

The sensitivity of the storage modulus of NORDEL IP 4520 (M_W=115,000)

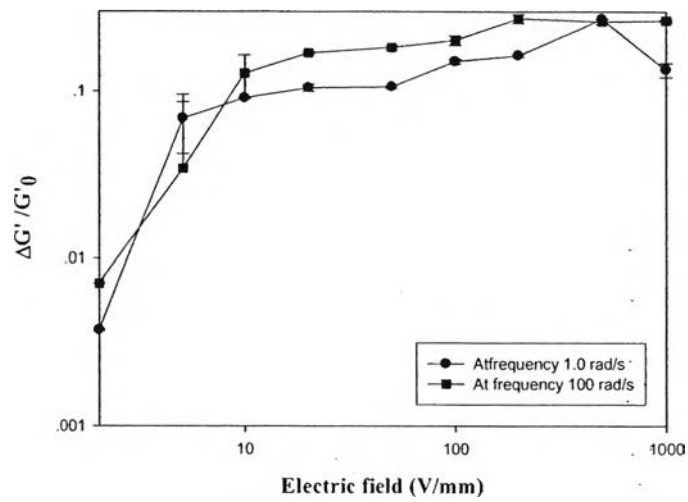

Figure G3 The sensitivity of the storage modulus □($\Delta G'/G'_0$) at T = 27°C, strain 0.2 %, vs. electric field strength (V/mm) of NORDEL IP 4520 ($G'_{0\ \text{at frequency 1.0 rad/s}}$=141,200 Pa and $G'_{0\ \text{at frequency 100 rad/s}}$=266,980 Pa).

Frequency test of NORDEL IP 4640 (M_W=160,000)

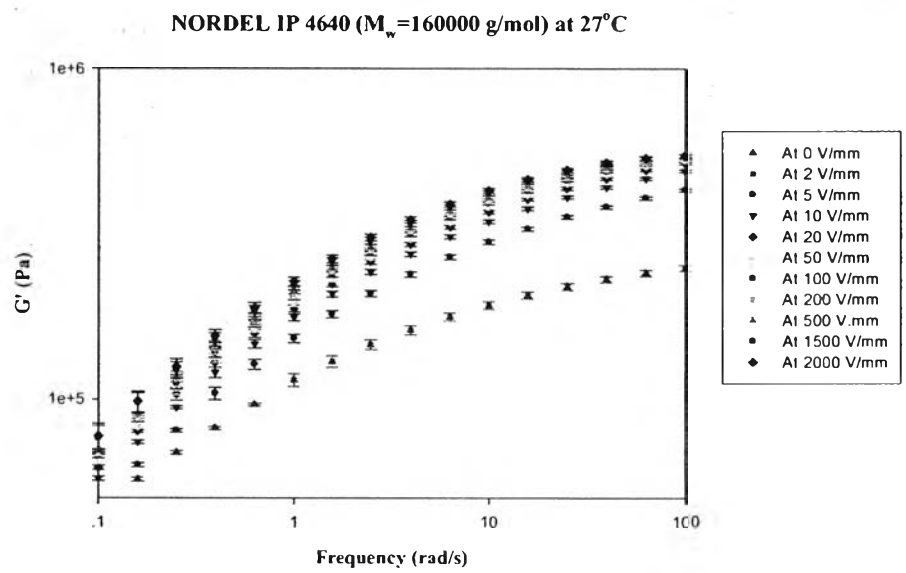

Figure G4 NORDEL IP 4640 at T = 27°C, strain 0.5 % frequency sweep test at various electric field strength (V/mm).

The storage modulus response of NORDEL IP 4640 (M_W=160,000)

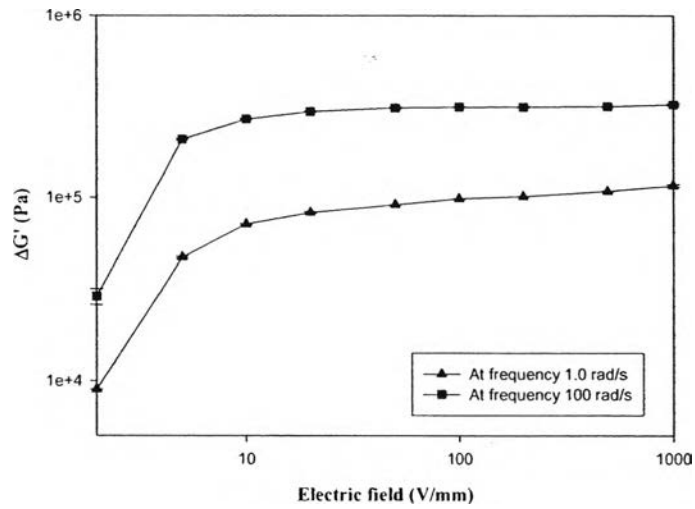

Figure. G5 The storage modulus response □(ΔG') at T = 27°C, strain 0.5 %, vs. electric field strength (V/mm) of NORDEL IP 4640.

The sensitivity of the storage modulus of NORDEL IP 4640 (M_W=160,000)

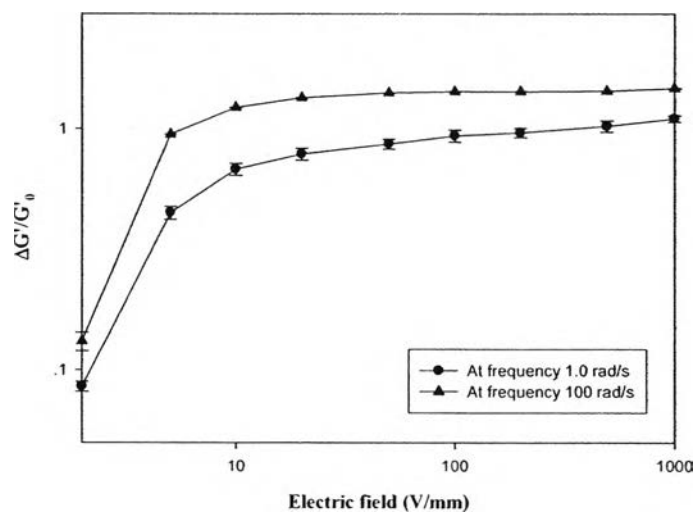

Figure G6 The sensitivity of the storage modulus □($\Delta G'/G'_0$) at T = 27°C, strain 0.5 %, vs. electric field strength (V/mm) of NORDEL IP 4640 ($G'_{0\ \text{at frequency 1.0 rad/s}}$=105,485 Pa and $G'_{0\ \text{at frequency 100 rad/s}}$=220,575 Pa).

Frequency test of NORDEL IP 4570 (M_W=210,000)

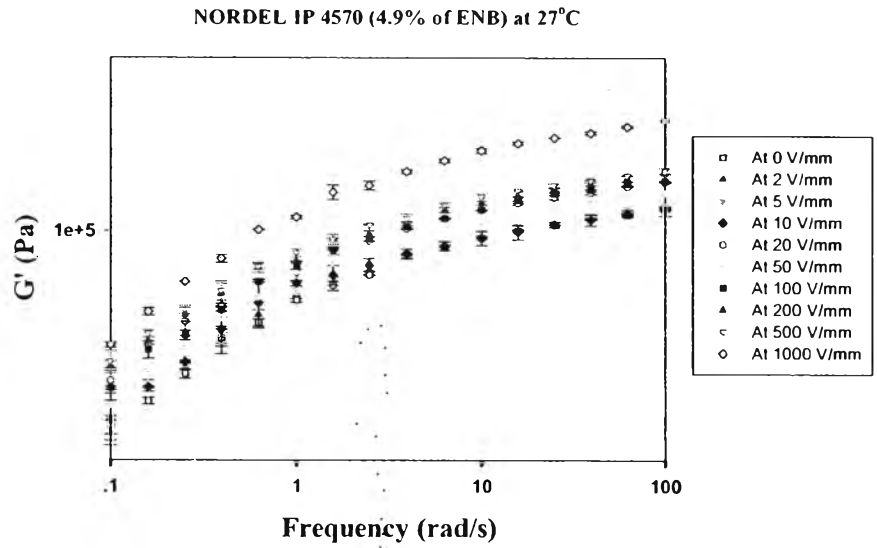

Figure G7 NORDEL IP 4570 at T = 27°C, strain 0.06 % frequency sweep test at various electric field strength (V/mm).

The storage modulus response of NORDEL IP 4570 (M_W=210,000)

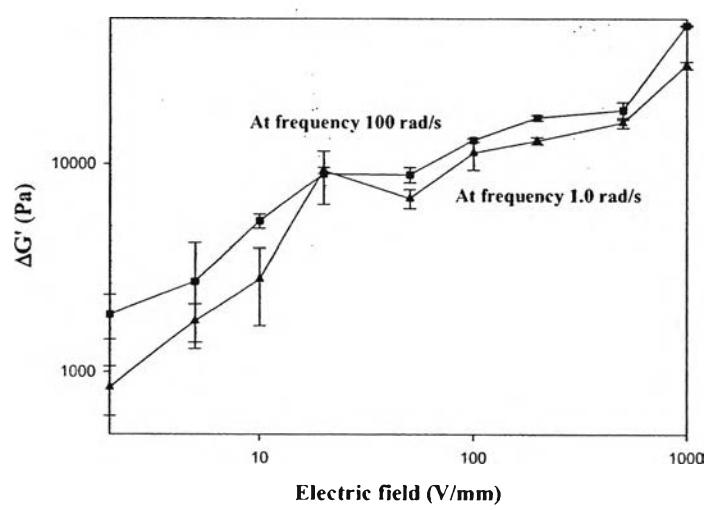

Figure G8 The storage modulus response (□ΔG') at T=27°C, and %strain=0.06, vs. electric field strength (V/mm) of NORDEL IP 4570.

The sensitivity of the storage modulus of NORDEL IP 4570 (M_w=210,000)

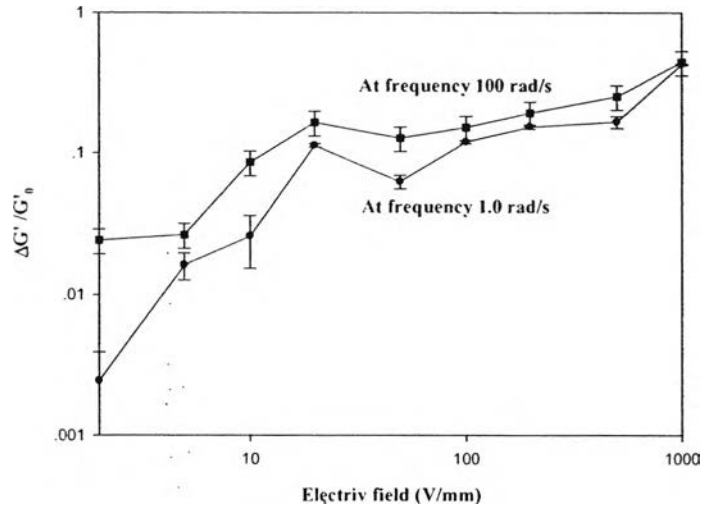

Figure G9 The sensitivity of the storage modulus □($\Delta G'/G'_0$) at T=27°C, and %strain=0.06, vs. electric field strength (V/mm) of NORDEL IP 4570 ($G'_{0 \text{ at frequency } 1.0 \text{ rad/s}}$=75,726.7 Pa and $G'_{0 \text{ at frequency } 100 \text{ rad/s}}$=109,220 Pa).

Appendix H Frequency Sweep Test; various electric fields and temperatures.

Frequency sweep test of pure EPDM with different ENB contents

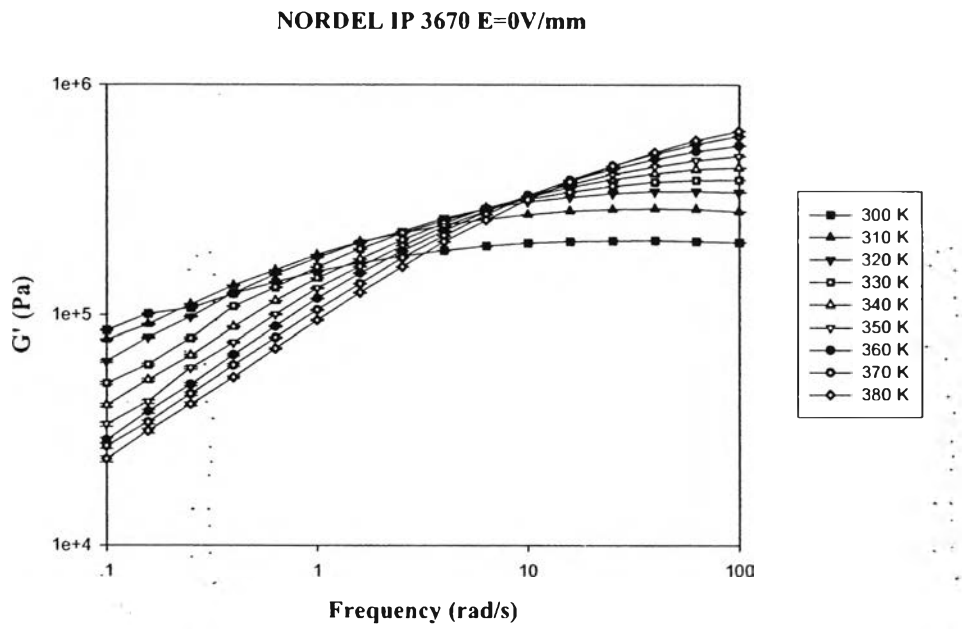

Figure H1 NORDEL IP 3670 at E = 0V/mm, gab=1.013 mm, strain 0.2 % in frequency sweep test at various temperatures.

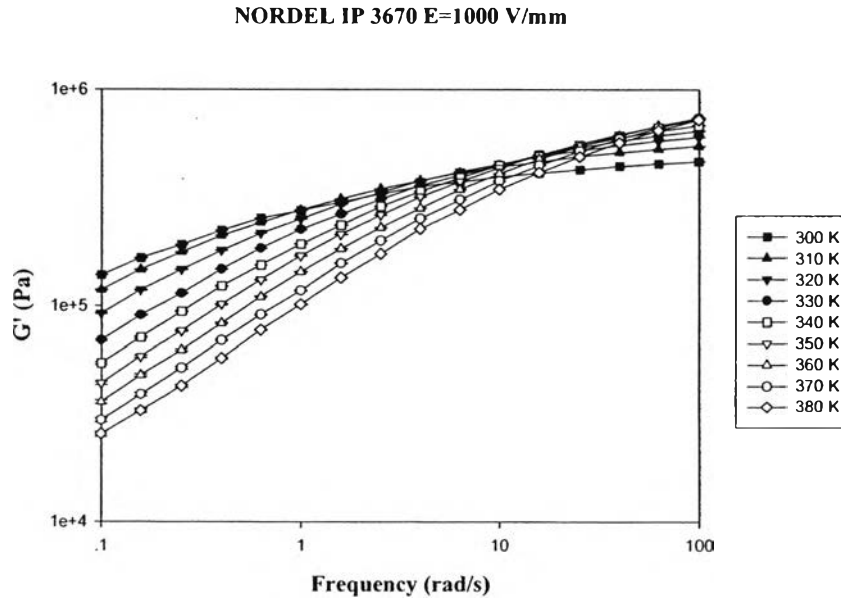

Figure H2 NORDEL IP 3670 at E = 1000V/mm, gab=1.001 mm, strain 0.2 % in frequency sweep test at various temperatures.

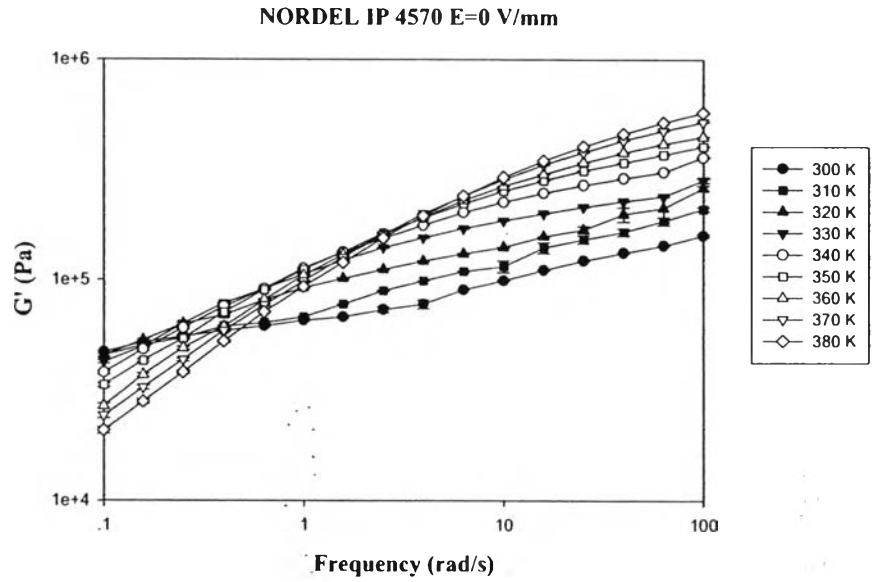

Figure H3 NORDEL IP 4570 at E = 0V/mm, gab=1.122 mm, strain 0.2 % in frequency sweep test at various temperatures.

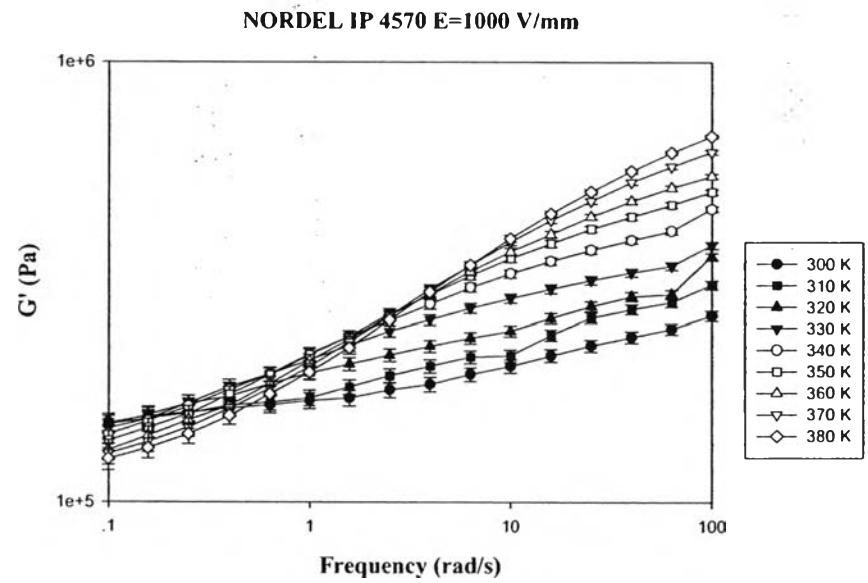

Figure H4 NORDEL IP 4570 at E = 1000V/mm, gab=0.995 mm, strain 0.3 % in frequency sweep test at various temperatures.

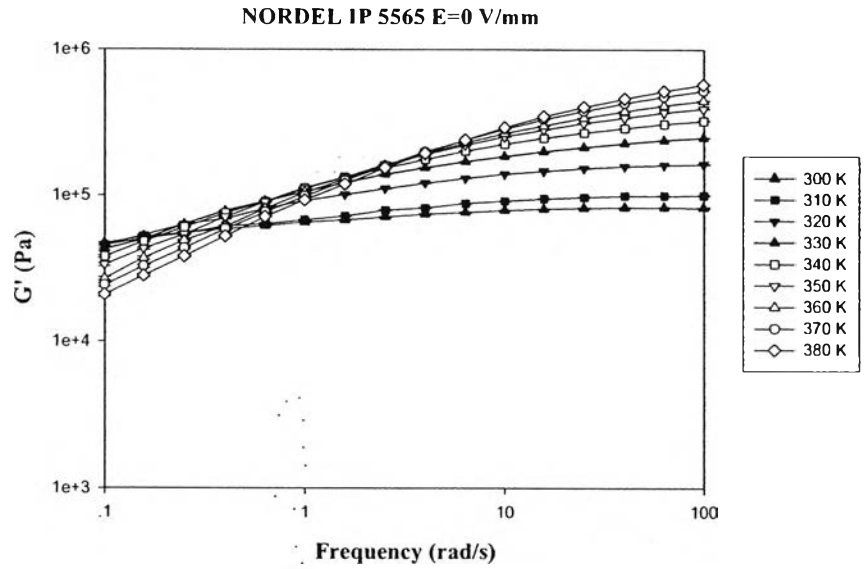

Figure H5 NORDEL IP 5565 at E = 0V/mm, gab=0,988 mm, strain 0.3 % in frequency sweep test at various temperatures.

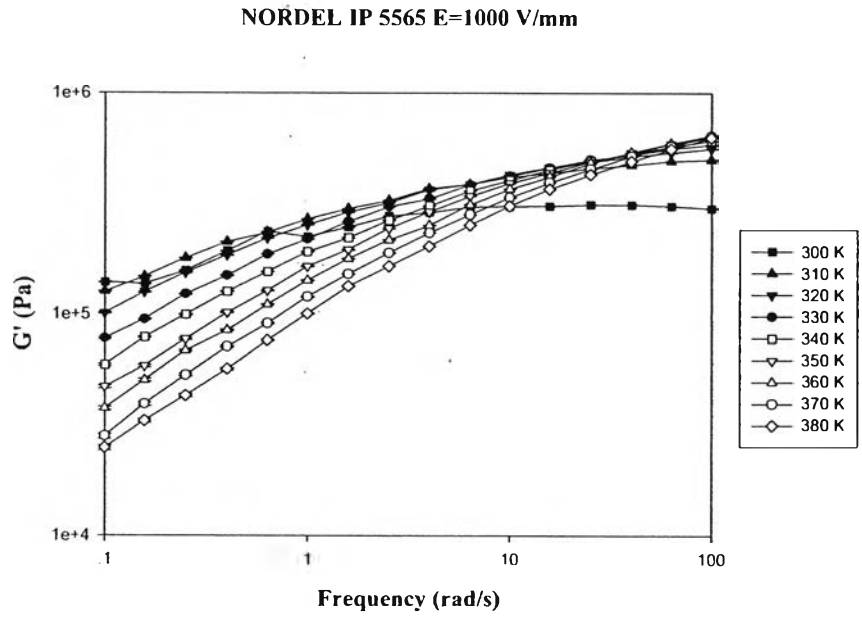

Figure H6 NORDEL IP 5565 at E = 1000V/mm, gab=1.011 mm strain 0.5 % in frequency sweep test at various temperatures.

Frequency sweep test of pure EPDM with different molecular weight contents

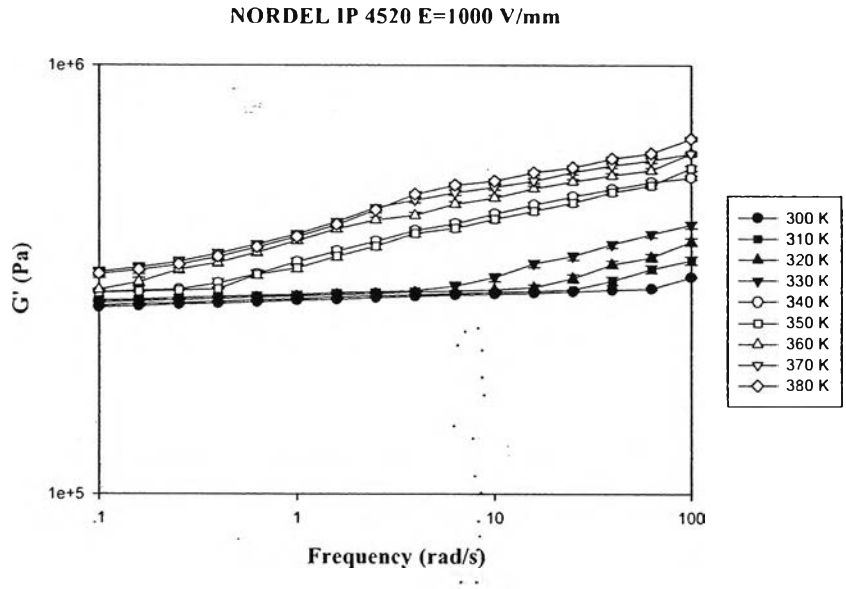

Figure H7 NORDEL IP 4520 at E = 0V/mm, gab=0.978 mm, strain 0.2 % in frequency sweep test at various temperatures.

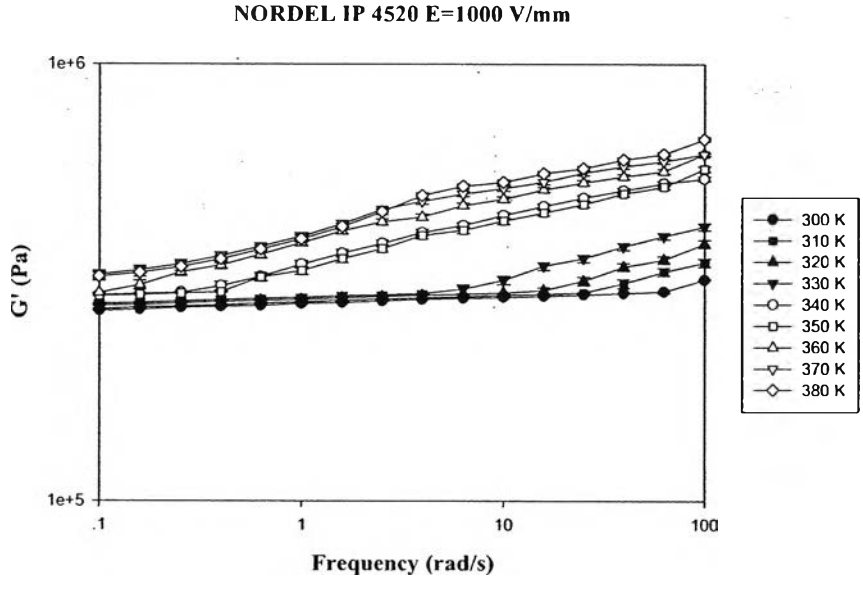

Figure H8 NORDEL IP 4520 at E = 1000V/mm, gab=0.878 mm, strain 0.4 % in frequency sweep test at various temperatures.

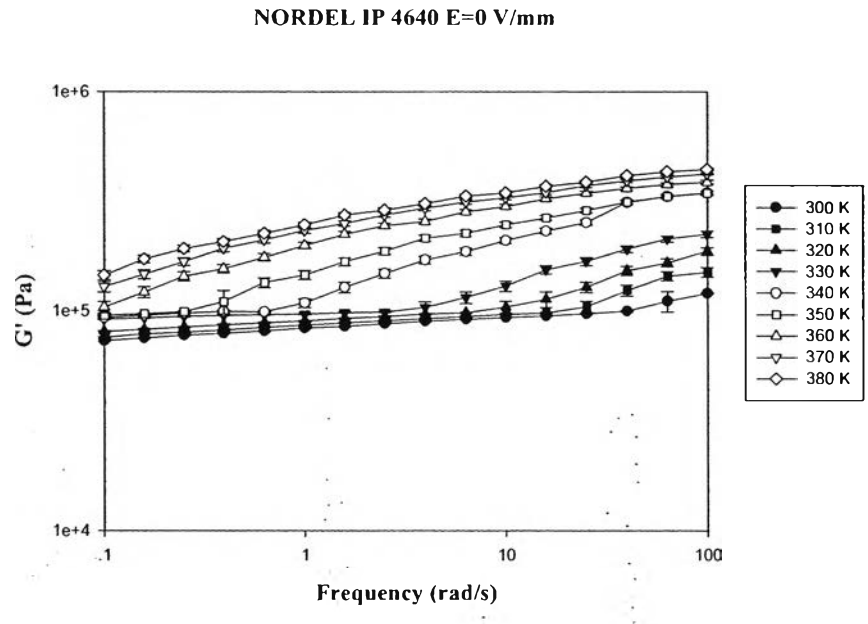

Figure H9 NORDEL IP 4640 at E = 0V/mm, gab=1.203 mm, strain 0.1 % in frequency sweep test at various temperatures.

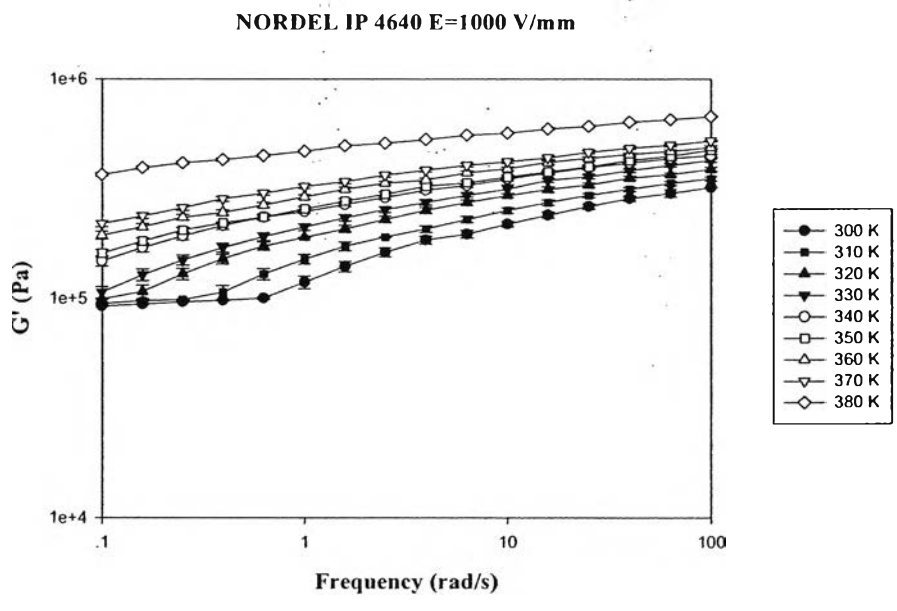

Figure H10 NORDEL IP 4640 at E = 1000V/mm, gab=1.143 mm strain 0.1 % in frequency sweep test at various temperatures.

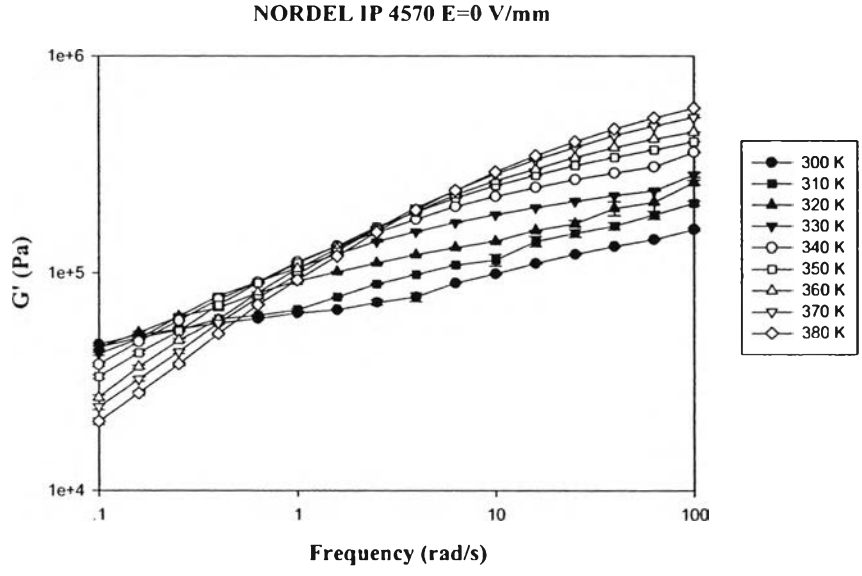

Figure H11 NORDEL IP 4570 at E = 0V/mm, gab=1.122 mm, strain 0.2 % in frequency sweep test at various temperatures.

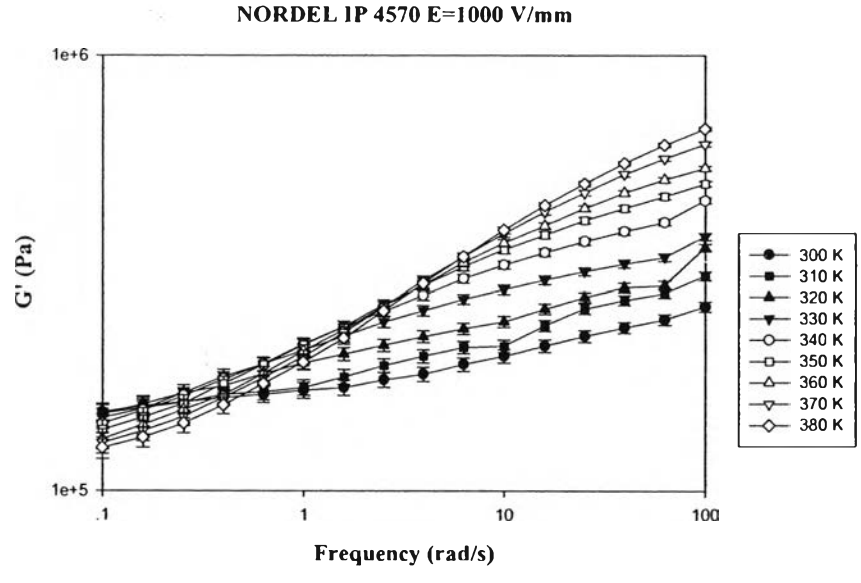

Figure H12 NORDEL IP 4570 at E = 1000V/mm, gab=0.995 mm, strain 0.3 % in frequency sweep test at various temperatures.

Appendix I The Storage Modulus of EPDM Films vs. Temperature at Various Electric fields.

The storage modulus of EPDM films with different ENB contents

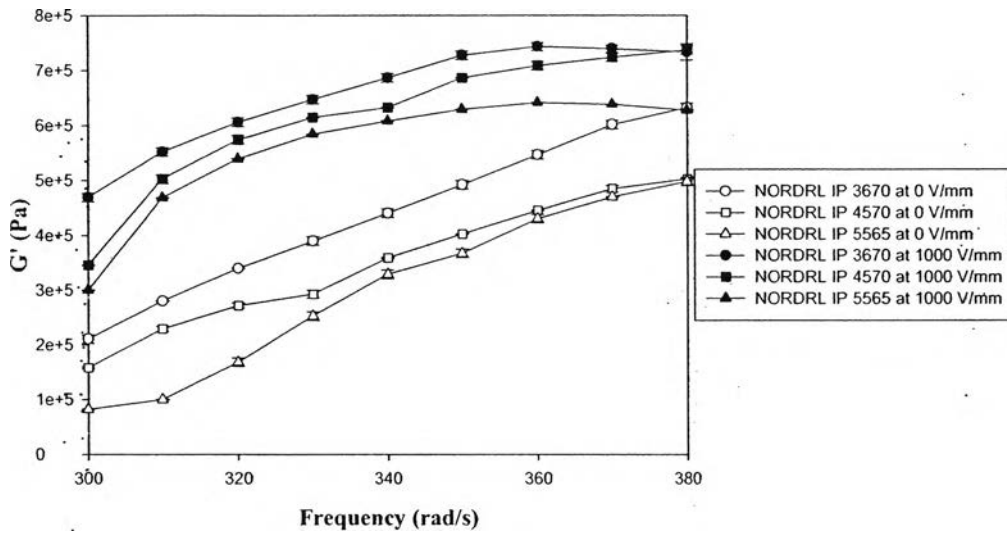

Figure I1 The storage modulus vs. temperature at the frequency 100 rad/s

Temperature (K)

The storage modulus of EPDM films with different molecular weight contents

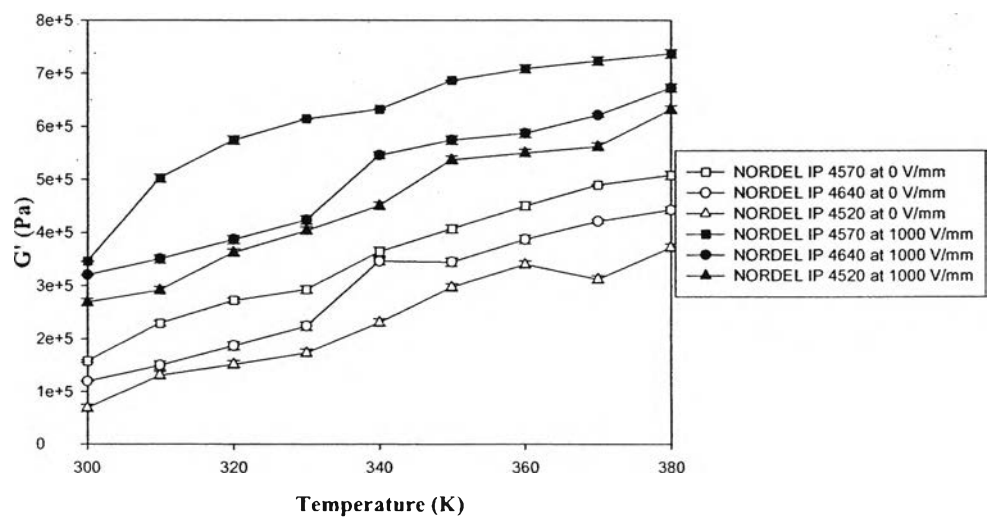

Figure I2 The storage modulus vs. temperature at the frequency 100 rad/s.

Appendix J Electromechanical Properties Measurement of Polymer Blends

Strain Sweep Test: polymer blend between permethylpolyazine PAZ and ethylene propylene diene rubber (NORFEL IP 5565) by using parallel plates

The temporal response of polymer blend films were carried out by melt rheometer meter (Rheometric Scientific, ARES). It was fitted with a custom-built copper parallel plates fixture, diameter 25 mm. A DC voltage was applied by DC power supply (Instek, GFG 8216A), which can deliver electric field strength to 1 kV/mm. A digital multimeter was used to monitor the voltage input. For temporal responses testing, oscillate shear strain was applied and the dynamic moduli (G' and G") were investigated as a function of time and electric field strength. Dynamic strain sweep test were first carried out to determine appropriate strains by measured G′ and G″ in linear viscoelastic regime. The following figures, Figure J1, J2, J3, and J4, show linear viscoelastic regimes of polymer blend films:, respectively, without electric field strength (0 V/mm). Besides, Figure J5, J6, J7, and J8, show the linear viscoelastic regimes of pure EPDM films in the influence of electric field strength at 1 kV/mm.

Table J1 Storage modulus and loss modulus data, obtained from dynamic strain sweep test of polymer blend (5%v/v of PAZ), parallel plate, gap = 0.876 mm, film diameter = 25 mm, electric field (E) = 0 V/mm, 27°C.

%Strain	G' (Pa)	G" (Pa)	%Strain	G' (Pa)	G" (Pa)
0.017	48097.3	12321.8	1.8688	47814.2	9125.31
0.0274	55465.7	11499	2.9628	47379.7	9479.34
0.0452	52439.2	11153.1	4.7034	46797.3	9869.23
0.0726	47639	8023.96	7.4653	45759	10633.8
0.1159	47555.1	8424.07	11.8807	43568.1	11401.9
0.1846	47587.1	8241.28	18.905	38395.4	10474.9
0.2935	46346.5	7744.18	30.0988	34928.7	11319.2
0.466	47163.3	7048.77	48.3169	26229.6	14088.1
0.7372	48204.6	8123.4	77.4166	18339.6	14020.6
1.1827	49281.1	6958.16	124.006	10489.5	11572.3

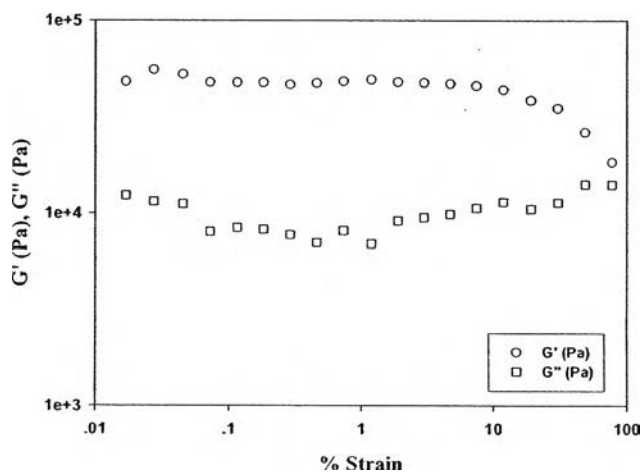

Figure J1 Storage modulus and loss modulus versus strain (%) obtained from dynamic strain sweep test of polymer blend (5%v/v of PAZ), parallel plate, gap = 0.876 mm, film diameter = 25 mm, electric field (E) = 0 V/mm, 27°C.

Table J2 Storage modulus and loss modulus data, obtained from dynamic strain sweep test of polymer blend (10%v/v of PAZ), parallel plate, gap = 0.858 mm, film diameter = 25 mm, electric field (E) = 0 V/mm, 27°C.

%Strain	G' (Pa)	G" (Pa)	%Strain	G' (Pa)	G" (Pa)
0.0194	37698.5	11700.6	1.897	38872.4	10971.3
0.0302	40793.3	9186.78	3.0092	38453.9	10949.4
0.0454	41344.4	10822.4	4.7748	37800.1	10877.7
0.0735	41048.1	11615.5	7.5851	36456.5	10942.1
0.1171	41607.3	10802.9	12.103	31851.8	11983.3
0.185	41205.1	10857.3	19.4654	20304.2	13406.2
0.2952	40881.6	11027	31.1002	14324.2	11981.2
0.4697	40308.6	11262	49.463	11168	8546.62
0.7476	39824.5	11163	78.4887	10020.1	5991.92
1.1954	39258.9	11088.3	124.42	8835.57	4101.93

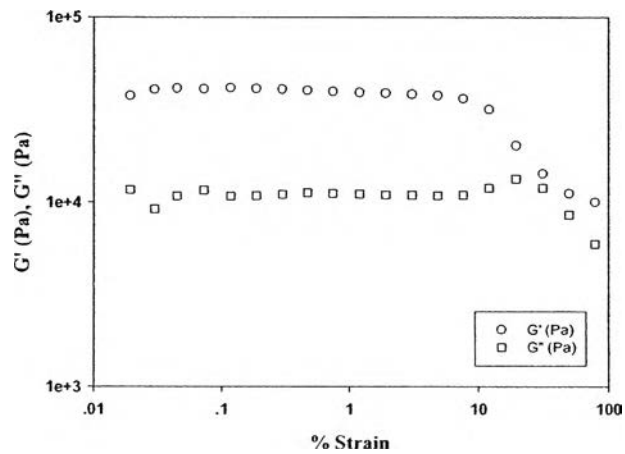

Figure J2 Storage modulus and loss modulus versus strain (%) obtained from dynamic strain sweep test of polymer blend (10%v/v of PAZ), parallel plate, gap = 0.858 mm, film diameter = 25 mm, electric field (E) = 0 V/mm, 27°C.

Table J3 Storage modulus and loss modulus data, obtained from dynamic strain sweep test of polymer blend (15%v/v of PAZ), parallel plate, gap = 0.921 mm, film diameter = 25 mm, electric field (E) = 0 V/mm, 27°C.

%Strain	G' (Pa)	G" (Pa)	%Strain	G' (Pa)	G" (Pa)
0.0164	92898.6	21675.9	1.6931	101690	28217.7
0.0256	100510	26731.4	2.6965	98736.3	28961.7
0.04	91359.7	19437.9	4.3063	93953.7	29520.2
0.0644	94526.7	20505.7	6.9592	80958.8	32465.6
0.1042	92348.7	20795	11.6156	44909.1	33983.9
0.1661	95957.3	22457.8	18.8513	32213.7	25268.3
0.2643	98945.8	21281.2	30.4476	21840.6	18541.4
0.4187	102450	23929.7	48.8781	14796	15436.7
0.6662	103440	25953.7	77.9992	10602	15529.1
1.0573	103450	27226.1	124.59	6355.74	12898

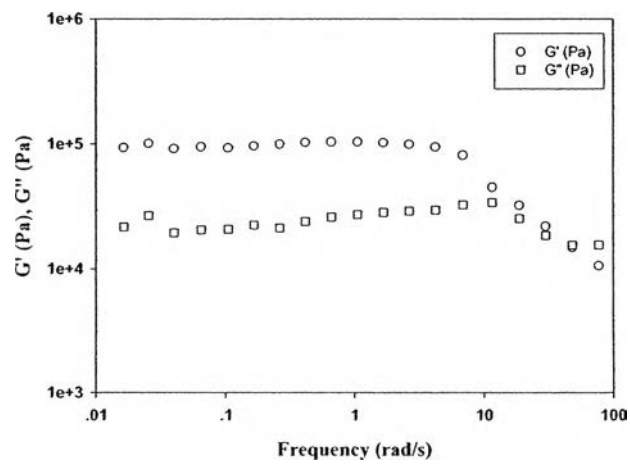

Figure J3 Storage modulus and loss modulus versus strain (%) obtained from dynamic strain sweep test of polymer blend (15%v/v of PAZ), parallel plate, gap = 0.915 mm, film diameter = 25 mm, electric field (E) = 0 V/mm, 27°C.

Table J4 Storage modulus and loss modulus data, obtained from dynamic strain sweep test of polymer blend (20%v/v of PAZ), parallel plate, gap = 0.873 mm, film diameter = 25 mm, electric field (E) = 0 V/mm, 27°C.

%Strain	G' (Pa)	G" (Pa)	%Strain	G' (Pa)	G" (Pa)
0.0184	61374.7	-2127.1	1.6816	109710	16010.4
0.0299	65287.6	10258.9	2.662	111240	21078.5
0.0459	70992.3	5516.1	4.2301	109460	25124.7
0.0691	73015.9	3521.53	6.734	100230	25207.6
0.1102	71613.8	2012.62	10.7739	94147.9	27061.2
0.1757	70574.8	6219.45	17.4724	79508.6	30470.8
0.2792	72383.5	4419	28.8546	53914	34958.3
0.4394	77485.6	4391.23	46.9438	38207.9	33694.5
0.6876	87096.6	5174.54	75.9459	25709.9	31832.1
1.0678	101690	8120.49	122.57	15582.7	25073.1

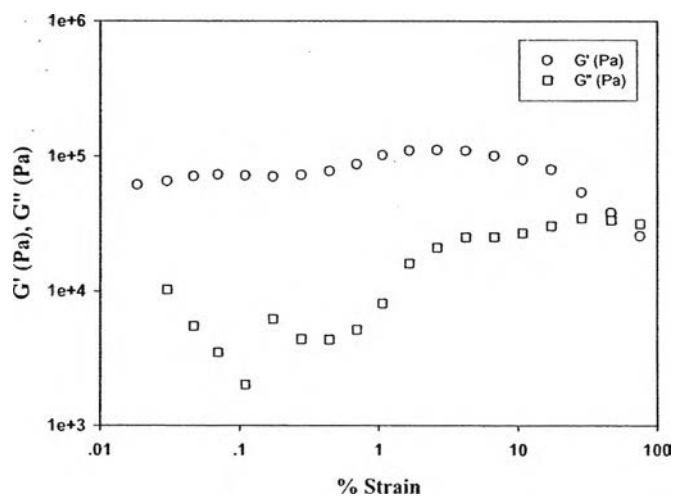

Figure J4 Storage modulus and loss modulus versus strain (%) obtained from dynamic strain sweep test of polymer blend (20%v/v of PAZ), parallel plate, gap = 0.873 mm, film diameter = 25 mm, electric field (E) = 0 V/mm, 27°C.

Table J5 Storage modulus and loss modulus data, obtained from dynamic strain sweep test of polymer blend (5%v/v of PAZ), parallel plate, gap = 0.786 mm, film diameter = 25 mm, electric field (E) = 1 V/mm, 27°C.

%Strain	G' (Pa)	G" (Pa)	%Strain	G' (Pa)	G" (Pa)
0.0185	47258.4	-2575	1.7354	105150	12730.7
0.0283	61086	6529.56	2.7367	109350	18287.3
0.0452	61442.7	12339.1	4.3304	110890	23017.9
0.0723	63535.1	9171.24	6.8903	101250	24652.2
0.1138	64125.7	9044.94	11.0151	94958.8	25247.3
0.1781	64807.4	10224.8	17.8712	78383.6	25570.4
0.2836	66231.4	9618.58	28.9539	61726.6	35854.3
0.4505	69898.6	9180.57	47.4738	39061.5	31555.7
0.7025	85176.4	6170.56	77.3218	18878	22519.5
1.1049	96372.3	7719.38	123.99	9517.58	14890.4

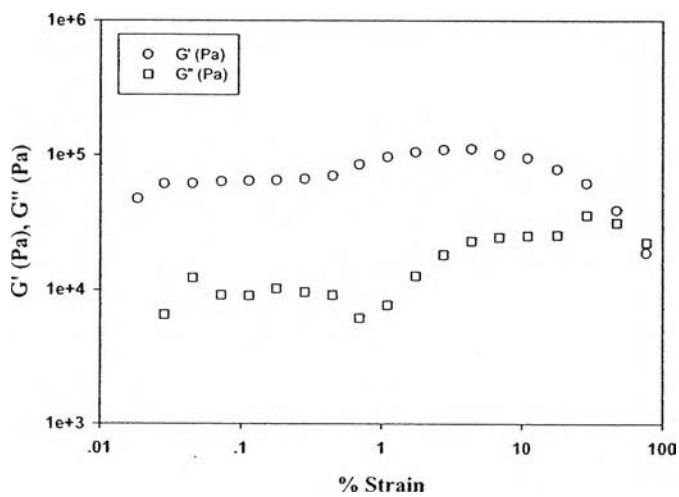

Figure J5 Storage modulus and loss modulus versus strain (%) obtained from dynamic strain sweep test of polymer blend (5%v/v of PAZ), parallel plate, gap = 0.786 mm, film diameter = 25 mm, electric field (E) = 1 V/mm, 27°C.

Table J6 Storage modulus and loss modulus data, obtained from dynamic strain sweep test of polymer blend (10%v/v of PAZ), parallel plate, gap = 0.841 mm, film diameter = 25 mm, electric field (E) = 1 V/mm, 27°C.

%Strain	G' (Pa)	G" (Pa)	%Strain	G' (Pa)	G" (Pa)
0.019	61244.7	13147.5	1.8384	64230.1	18112.4
0.03	62204.1	14364.6	2.9132	64236.7	18373.5
0.0468	63632.8	15585.2	4.6255	63245	18673.5
0.0719	64823.9	18219.9	7.4054	55067.1	21500.3
0.1139	64496.5	17212.5	11.9834	39071.5	23140.8
0.183	63806.1	16500.9	19.3527	24847	19593.5
0.2901	63679.8	17368	31.078	14001.2	11848.2
0.4573	64359	17845.2	49.5246	10129.1	8592.78
0.7252	64688.1	17880.3	78.7194	8753.05	5801.54
1.1582	64331.1	17978.9	123.767	12144.1	6170.83

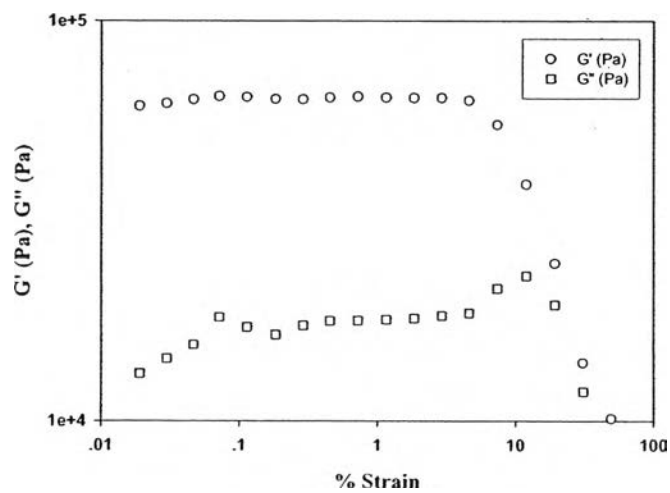

Figure J6 Storage modulus and loss modulus versus strain (%) obtained from dynamic strain sweep test of polymer blend (10%v/v of PAZ), parallel plate, gap = 0.841 mm, film diameter = 25 mm, electric field (E) = 1 V/mm, 27°C.

Table J7 Storage modulus and loss modulus data, obtained from dynamic strain sweep test of polymer blend (15%v/v of PAZ), parallel plate, gap = 0.758 mm, film diameter = 25 mm, electric field (E) = 1 V/mm, 27°C.

%Strain	G' (Pa)	G" (Pa)	%Strain	G' (Pa)	G" (Pa)
0.0164	125270	22582.2	1.6167	123170	37684.3
0.0268	121060	28328.1	2.586	118230	38176.5
0.0417	124600	26975.8	4.1466	110980	38126
0.065	124600	24170.6	6.6968	93390.4	35607.4
0.1027	124420	32296.1	11.3006	56652.1	40010.7
0.1616	127640	33099.3	18.5663	37356.9	30077.5
0.2546	127230	33425.2	30.2796	22933.2	21877.4
0.4015	127490	35028.8	48.4558	18256.6	17628.2
0.6345	128250	35832.4	77.7343	13057	17616.7
1.0089	126520	37152.7	124.092	7980.01	14768.2

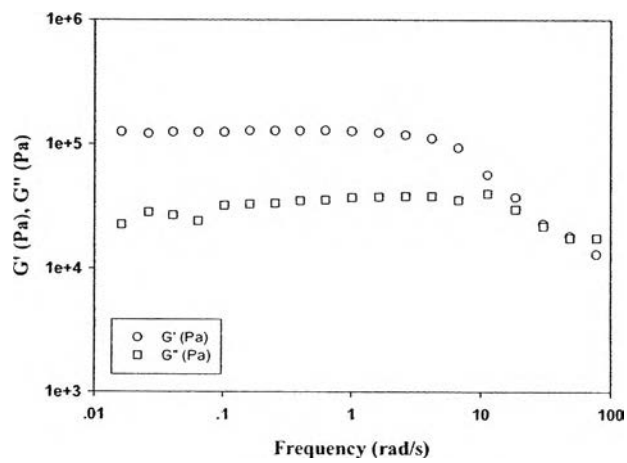

Figure J7 Storage modulus and loss modulus versus strain (%) obtained from dynamic strain sweep test of polymer blend (15%v/v of PAZ), parallel plate, gap = 0.758 mm, film diameter = 25 mm, electric field (E) = 1 V/mm, 27°C.

Table J8 Storage modulus and loss modulus data, obtained from dynamic strain sweep test of polymer blend (20%v/v of PAZ), parallel plate, gap = 0.737 mm, film diameter = 25 mm, electric field (E) = 1 V/mm, 27°C.

%Strain	G' (Pa)	G" (Pa)	%Strain	G' (Pa)	G" (Pa)
0.0178	106870	7904.77	1.5253	172830	34206.3
0.0268	117220	-2420.6	2.4232	170890	39941.4
0.0426	114430	-5353	3.8903	152340	39709.7
0.0679	108190	1752.75	6.2478	143540	39551.5
0.1062	108720	8655.85	9.998	137090	39979
0.1645	115200	2165.2	16.3508	116910	45855.5
0.2572	123500	5880.6	27.573	77086.9	51680.4
0.3996	140580	7123.49	46.1221	45323.2	49114
0.6147	158570	16756.8	75.1306	30106.8	42686.3
0.9603	169560	25755.4	121.768	18037.2	30950.5

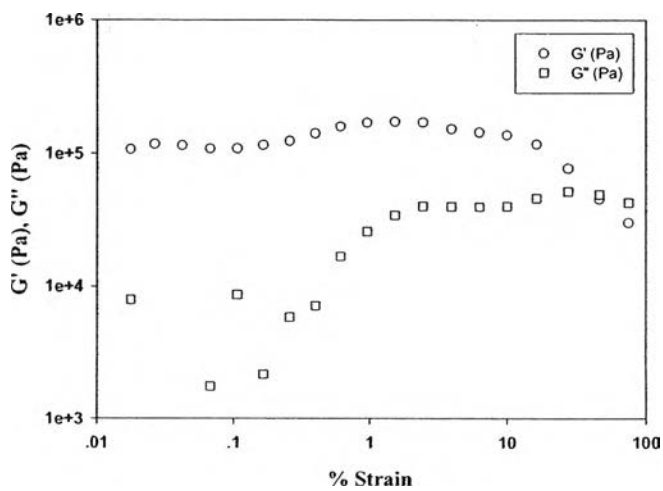

Figure J8 Storage modulus and loss modulus versus strain (%) obtained from dynamic strain sweep test of polymer blend (20%v/v of PAZ), parallel plate, gap = 0.737 mm, film diameter = 25 mm, electric field (E) = 1 V/mm, 27°C.

Appendix K Frequency Sweep Test of Polymer Blend; various electric fields.

Frequency sweep test of polymer blend: 5%v/v of PAZ

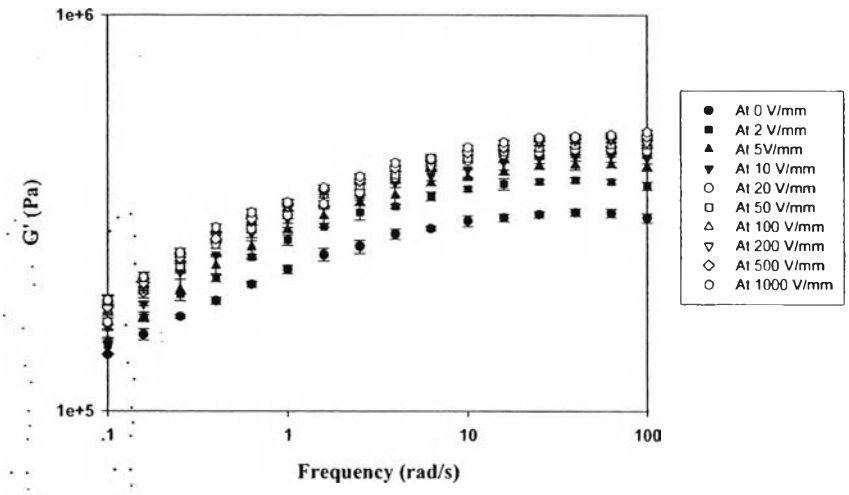

Figure K1 Polymer blend: 5%v/v of PAZ at 27°C, strain 1.0% in frequency sweep test mode at various electric field strengths (V/mm).

The storage modulus response (ΔG') and sensitivity (ΔG'/G'$_0$) of polymer blend: 5%v/v of PAZ

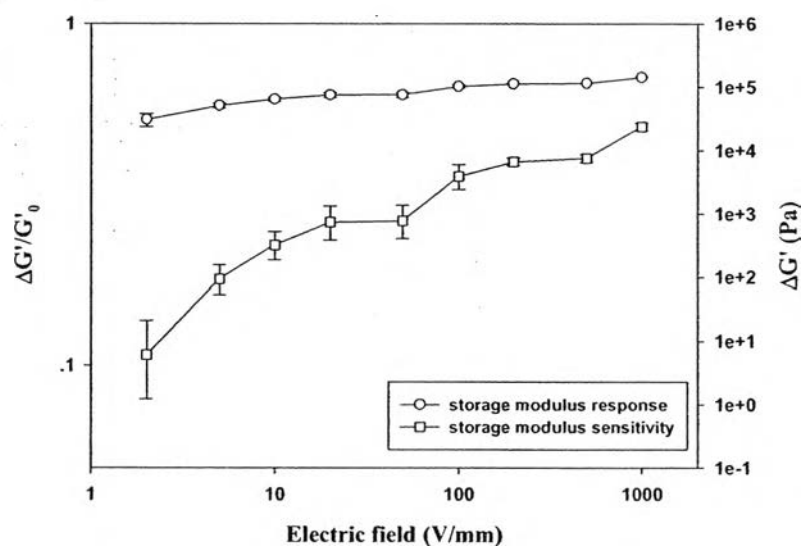

Figure K2 The storage modulus response (ΔG') and sensitivity (ΔG'/G'$_0$) of polymer blend: 5%v/v of PAZ, ω=100 rad/s at various electric field strengths (V/mm).

Frequency sweep test of polymer blend: 10%v/v of PAZ

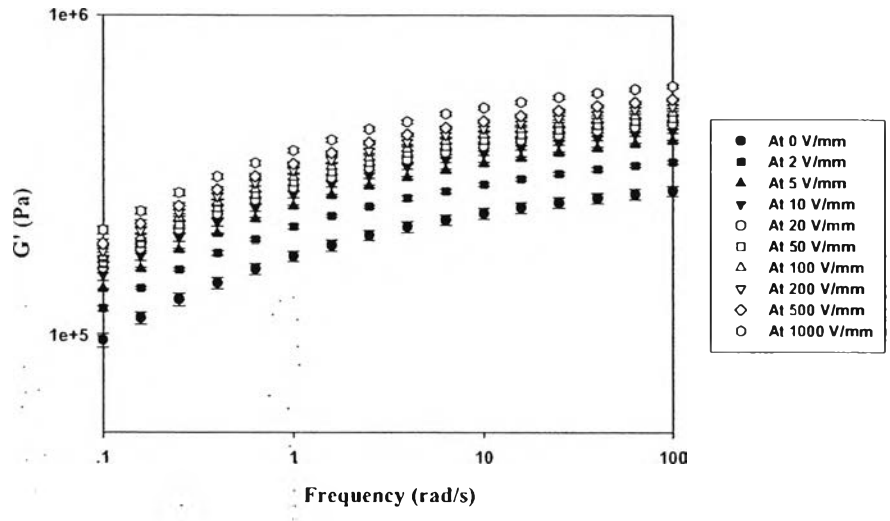

Figure K3 Polymer blend: 10%v/v of PAZ at 27°C, strain 1.0% in frequency sweep test mode at various electric field strengths (V/mm).

The storage modulus response (ΔG') and sensitivity (ΔG'/G'$_0$) of polymer blend: 10%v/v of PAZ

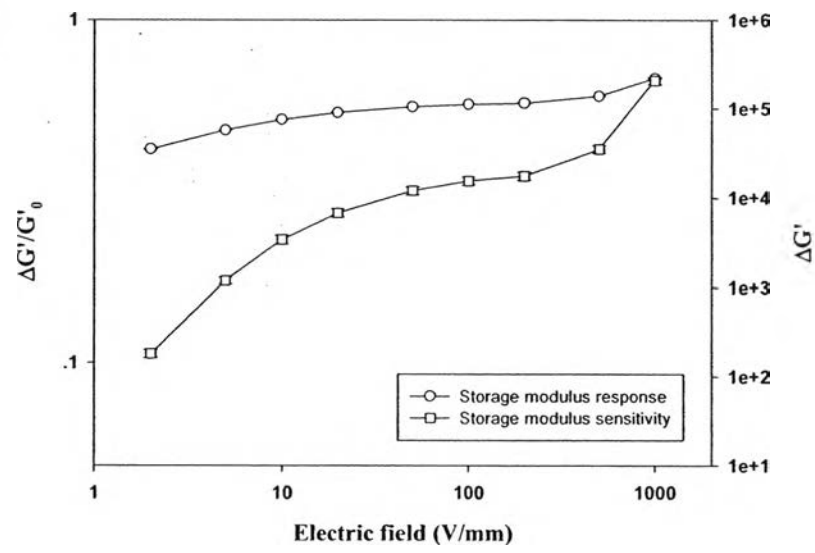

Figure K4 The storage modulus response (ΔG') and sensitivity (ΔG'/G'$_0$) of polymer blend: 10%v/v of PAZ, ω=100 rad/s at various electric field strengths (V/mm).

Frequency sweep test of polymer blend: 15%v/v of PAZ

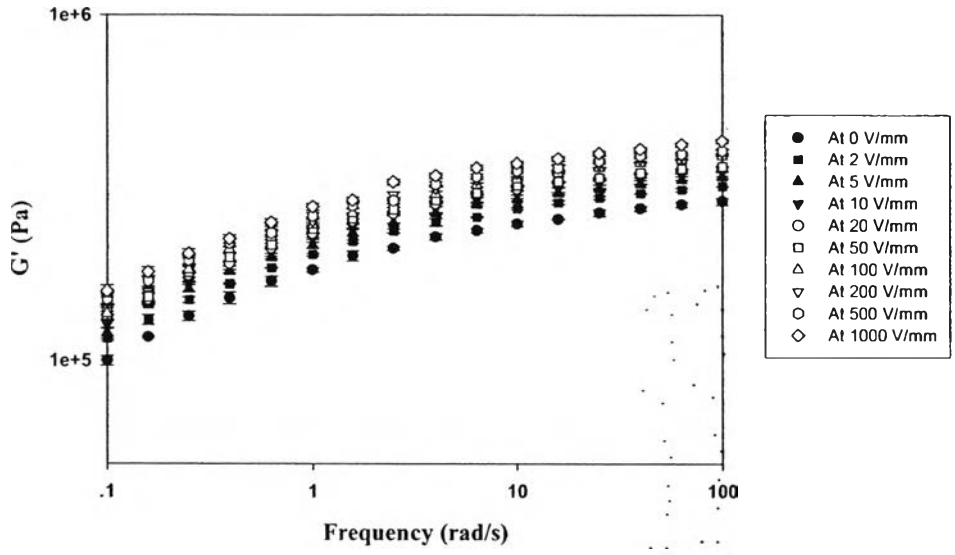

Figure K5 Polymer blend: 15%v/v of PAZ at 27°C, strain 1.0% in frequency sweep test mode at various electric field strengths (V/mm).

The storage modulus response (ΔG') and sensitivity (ΔG'/G'$_0$) of polymer blend: 15%v/v of PAZ

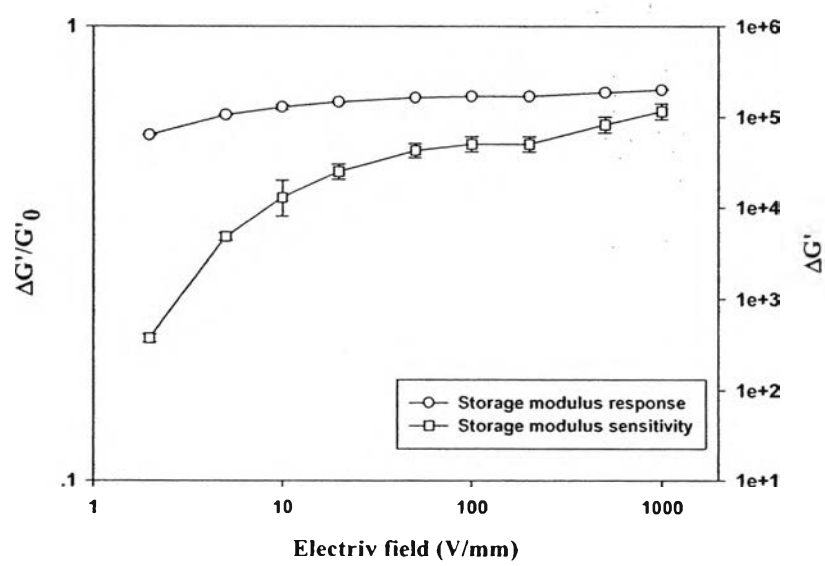

Figure K6 The storage modulus response (ΔG') and sensitivity (ΔG'/G'$_0$) of polymer blend: 15%v/v of PAZ, ω=100 rad/s at various electric field strengths (V/mm).

Frequency sweep test of polymer blend: 20%v/v of PAZ

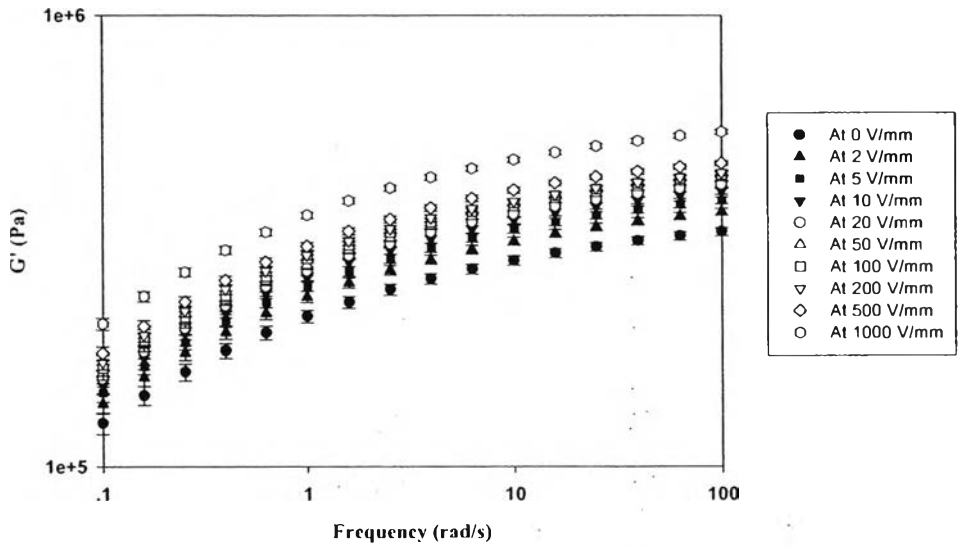

Figure K7 Polymer blend: 20%v/v of PAZ at 27°C, strain 1.0% in frequency sweep test mode at various electric field strengths (V/mm).

The storage modulus response ($\Delta G'$) and sensitivity ($\Delta G'/G'_0$) of polymer blend: 20%v/v of PAZ

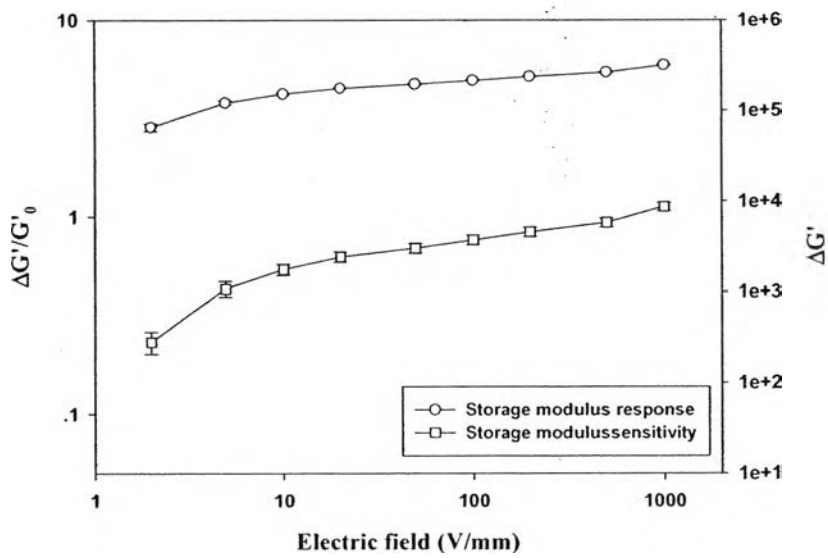

Figure K8 The storage modulus response ($\Delta G'$) and sensitivity ($\Delta G'/G'_0$) of polymer blend: 20%v/v of PAZ, ω=100 rad/s at various electric field strengths (V/mm).

CURRICULUM VITAE

Name: Ms. Patcharee Intanoo

Date of Birth: July 6, 1985

Nationality: Thai

University Education:

2004–2007 Bachelor Degree of Industrial Chemistry, Faculty of Science, Chiang Mai University, Chiang Mai, Thailand

Proceedings:

1. Intanoo, P.; Sirivat, A. (2010, April 22) Electromechanical Properties of Permethylpolyazine-Ethylene Propylene Diene Elastomer Blends. Proceedings of the 1st National Research Symposium on Petroleum, Petrochemicals, and Advanced Materials and The 16th PPC Symposium on Petroleum, Petrochemicals, and Polymers, Bangkok, Thailand.

Presentations:

1. Intanoo, P.; Sirivat, A. (2010, April 22) Electromechanical Properties of Permethylpolyazine-Ethylene Propylene Diene Elastomer Blends. Paper presented at the 1st National Research Symposium on Petroleum, Petrochemicals, and Advanced Materials and The 16th PPC Symposium on Petroleum, Petrochemicals, and Polymers, Bangkok, Thailand.